CHALMERS
UNIVERSITY OF TECHNOLOGY

Evaluation of Converting an AC Distribution Cabinet to DC Operation

Technical Consequences of Converting AC Distribution Cabinets to DC

Master's thesis in Sustainable Electric Power Engineering and Electromobility

DANIEL FATHI

DEPARTMENT OF ELECTRICAL ENGINEERING
CHALMERS UNIVERSITY OF TECHNOLOGY

Gothenburg, Sweden 2026
www.chalmers.se

Master's thesis 2026

Evaluation of Converting an AC Distribution Cabinet to DC Operation

Technical Consequences of Converting AC Distribution Cabinets to DC

Daniel Fathi

CHALMERS
UNIVERSITY OF TECHNOLOGY

Department of Electrical Engineering
Division of Electric Power Engineering
Chalmers University of Technology
Gothenburg, Sweden 2026

DC Applications in Low-Voltage Distribution Systems
Technical Consequences of Converting AC Distribution Cabinets to DC
Daniel Fathi

Supervisor: Niclas Fogelberg, ABB Alingsås
Examiner: Torbjorn Thiringer, Chalmers University

Master's Thesis 2026

Department of Electrical Engineering
Division of Electric Power Engineering
Chalmers University of Technology
SE-412 96 Gothenburg
Telephone +46 31 772 1000

Cover: Illustration of low-voltage distribution system analysis.

Typeset in LaTeX
Printed by Chalmers Reproservice
Gothenburg, Sweden 2026

Chalmers University of Technology

Abstract

These days, the rapid growth of loads based on direct current has increased quickly. Loads such as EV chargers, photovoltaic systems, energy storage systems, and power electronic equipment have made the use of DC distribution systems at the low-voltage level more important. DC system helps to avoid several conversion of AC/DC conversion, which reduces losses, makes the system simpler, and increases the overall efficiency.

In this thesis, the consequences of converting a three-phase AC cabinet to a proposed bipolar DC structure cabinet have been investigated. A comparison between these two systems has been performed in terms of power transfer, power losses, thermal behavior, efficiency, insulation stress, cable structure, protection, and environmental impacts.

The results show that the DC structure can transfer higher active power at the same rated current, and also, because of using fewer conductors and removing effects such as reactive power and power factor, the conduction losses in the system are reduced, which leads to lower temperature inside the cabinet and higher overall system efficiency. Despite these advantages, converting the AC system to DC has challenges such as DC protection, the lack of natural zero crossing of the current, electric arc extinction and fault current interruption.

Overall, the results of this thesis indicate that converting a low-voltage AC distribution cabinet to DC is a practical and achievable solution for future distribution networks.

Contents

1

Introduction

1.1 Background

Electrification has grown very fast in many different areas, for instance in buildings, commercial systems, renewable energy, energy storage and microgrids. Today we have many loads such as power electronic devices, electric vehicle chargers, renewable energy sources, photovoltaic systems, and energy storage systems (batteries) that work in direct current (DC). Therefore, today we have a high demand for direct current (DC) at the low-voltage distribution level.

ABB has been producing and designing cabinets for 400V three-phase AC in low voltage distribution for almost 100 years. As more DC based loads are connected to the AC system, we need more AC/DC conversion stages, these extra conversions lead to extra energy losses, more system complexity, and lower efficiency. However, the increasing of demand for DC applications has now motivated ABB to see how an AC based cabinet can be adapted to DC low voltage distribution operation.

Several studies have shown that low voltage DC distribution has advantages such as lower losses, better overall efficiency especially in the lower parts of the network and close to the end users, simpler system structure, material usage and higher power transform capability[5],[8].

At the same time, converting an AC cabinet to DC cabinet is not simple, there are many things that need to be considered, such as protection, safety, thermal, design and standardization. So, based on this background, we need also to study how a low voltage AC distribution systems more in general can be converted into low voltage DC distribution systems[2].

1.2 Previous Work

Many studies have focused on use of low-voltage DC distribution systems as an alternative instead of AC systems, especialy in applications with high power electronic loads. Research has shown that, DC systems have higher efficiency, lower transmission losses, and have a better compatibility with renewable energy storage systems due to their DC structure.

In previous work, it has been shown that DC systems have many benefits in buildings, data centers, microgrids, and electric vehicle charging infrastructure[3],[5],[10]. Furthermore, improvements in power electronics are another reason that make the AC to DC conversion more efficient and popular.

1.3 Purpose

The purpose of this thesis is to analyze the technical consequences of converting a low voltage AC distribution cabinet to a low voltage DC distribution cabinet. The AC system will be used as a benchmark, and the goal is to clearly show how switching from AC to DC have affect on current levels, thermal behavior, power transfer capability, losses and safety and overall system design.

The outcome of this thesis is to identify the consequences of moving from an AC cabinet to a DC cabinet, So, that this work will be expected to give a clearer understanding of how DC system have changed in terms of electrical behavior, losses, thermal performance, safety, and material usage.

1.4 Limitations and Delimitations

There are two main limitations in this thesis. The first limitation is related to the short-circuit test in the DC cabinet. Due to laboratory limitations, it was not possible to perform short-circuit tests on the DC system.

The second limitation is the lack of installation of the DC switch-disconnector. To install switch like OTDC switch on the ABB busbars, an adapter is needed that can be placed between the switch disconnector and the busbars. The existing adapters are designed for the AC system, but they do not exist for the DC system. Therefore, a DC adapter is needed for installing this equipment.

2
Theoretical Background

In this section, the theoretical concepts which are used in this thesis will be present. It explains the theories and formulas related to power transfer, electrical losses, and thermal behavior in both AC and DC systems. It also gives a short overview of the DC distribution topology and briefly discusses the main protection challenges in DC systems.

2.1 Power Transfer and Current in AC and DC Systems

For a three-phase AC system, the transmitted active power can be defined as

$$P_{AC,3\phi} = \sqrt{3}\, V_{LL}\ I_L\ \cos\phi$$

where V_{LL} is the line-to-line voltage, I_L is the line current, and $\cos\phi$ is the power factor. The factor $\sqrt{3}$ comes from the relation between line and phase values in a three-phase system.

For a single-phase AC system, the active power can be defined as

$$P_{AC} = V\ I\ \cos\phi$$

The transmitted active power in a DC system can be written as

$$P_{DC} = V_{DC}\ I_{DC}$$

where V_{DC} is the DC voltage and I_{DC} is the DC current.

In AC systems, the current is alternating and there is frequency, reactive power, and power factor.

In DC systems, the current is direct and there is no frequency, reactive power, and power factor. So, all the current is used to transfer the active power. This leads to improved conductor efficiency and higher power transfer capability.

2.2 Power Losses in Conductors

The resistance in the conductors, which opposes the flow of current, causes power losses.

For DC systems it can be written as

$$P_{loss,DC} = I_{DC}^2 R_{DC}$$

For AC systems it can be written as

$$P_{loss,AC} = I_{rms}^2 R_{AC}$$

Because of the characteristics of AC and DC systems, their effective conductor resistances are different. In AC systems, the resistance is higher than in DC systems. This is due to the skin effect, where the current tends to concentrate near the surface of the conductor.

2.3 Thermal Behavior

Electrical losses in conductors and electrical components turn into heat during operation, which leads to a temperature rise in the system. Therefore, the temperature rise in an electrical system directly depends on the generated losses and the thermal resistance of the system.

$$\Delta T = P_{loss} R_{th}$$

where P_{loss} is the generated power loss and R_{th} is the thermal resistance of the system.

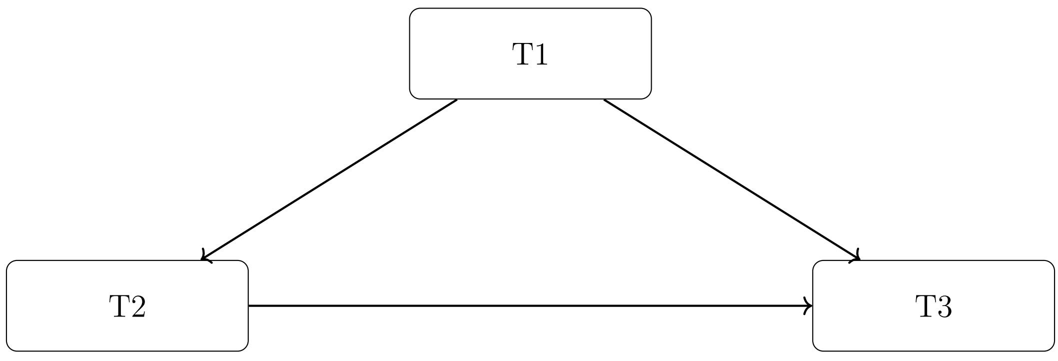

Figure 2.1: Heat transfer paths

For larger networks, the relation can be written in matrix form as

$$\begin{bmatrix} \Delta T_1 \\ \Delta T_2 \\ \Delta T_3 \end{bmatrix} = \begin{bmatrix} R_{11} & R_{12} & R_{13} \\ R_{21} & R_{22} & R_{23} \\ R_{31} & R_{32} & R_{33} \end{bmatrix} \begin{bmatrix} P_1 \\ P_2 \\ P_3 \end{bmatrix}$$

2.4 Protection and Safety in AC and DC Systems

Protection principles are different between AC and DC systems. In AC systems, the current naturally crosses zero twice per cycle. This zero-crossing helps circuit breakers extinguish the arc and makes fault interruption easier.

In DC systems, there is no natural current zero-crossing. During faults, the current rises quickly and continues to flow, which makes arc extinction more difficult. Because of this, DC systems require Fast-acting circuit breakers, Hybrid or solid-state breakers and Advanced fault detection and coordination strategies.

2.5 DC Distribution Topologies

In DC systems, the power distribution structure exists in two types, unipolar and bipolar.

unipolar Topology

In the unipolar structure, power transfer is carried out only through two conductors, positive and negative, and the system is simple in terms of structure and design, but its flexibility and reliability are more limited. In this structure, there is only one main path for power transfer, so in case of a fault or problem, the entire system is affected. Also, since the entire current flows through a single path, the possible losses can be high [35].

Bipolar Topology

The bipolar structure consists of three conductors, which include the positive pole, negative pole, and a neutral conductor (±DC with neutral). In this structure, power can be distributed between the positive and negative poles, each pole can have 380 V with respect to neutral, and the voltage difference between the positive and negative poles reaches 760 V DC.

This system (±DC with neutral) supports flexible load connection by allowing pole-to-pole and pole-to-neutral connections. This topology makes the system more practical and improves the utilization of the conductors, especially when there are unbalanced loads. Voltage levels in low-voltage DC applications include 24 V, 48 V, 380 V, and ±760 V [36].

3

Case Definition

3.1 Case Study Definition

This section describes the case study that has been used in this thesis. It introduces the reference AC distribution cabinet and the proposed DC alternative that will be studied in this work. The objective is to define the main electrical and physical parameters of the system that will be used as the basis for the following analysis.

Reference AC Distribution Cabinet

Product Definition

The reference case is an ABB low-voltage cabinet (Kabeldon SDC 1673) that is designed for outdoor applications. The cabinet uses a four-wire busbar system (L1, L2, L3 and N) conductors, and the cabinet rated is a nominal line-to-line voltage of 400 V and rated current of 1600 A.

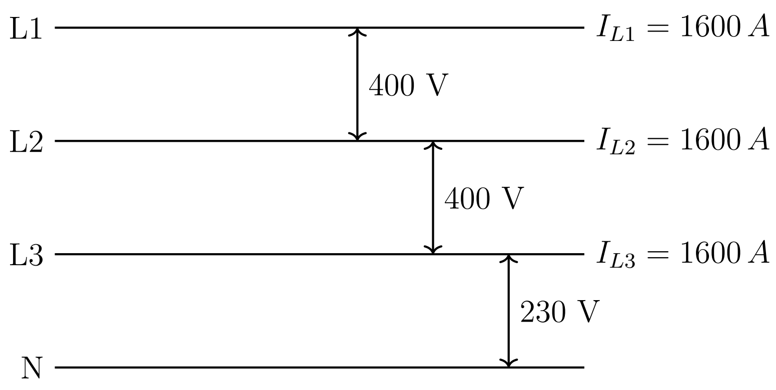

Figure 3.1: Three-phase AC busbar system

Main Components Inside the Cabinet

Inside this cabinet, the main components are

- Three phase busbars (KSFS 1698), used as phase conductors.
- One neutral / protective earth busbar (KSNS 1098), used for N and PE connections.
- Busbar supports (KSST 316/23), used to hold the busbars in place and act as insulation between the busbars and the cabinet.
- Fuse switch disconnector, SLE 2, used for outgoing feeders with NH size 2 fuses (400 A).
- Cable connection interfaces (ADI 300), used to connect incoming cables to the busbar system.

Figure 3.2: Internal structure of the AC distribution cabinet.

As shown in Fig. 3.3, the Cable distribution cabinet is located between the power source and the loads. It receives power from the AC grid through an underground cable and distributes it to several loads. The cabinet operates as a distribution node between the source and the loads [20].

Electrical System

Table 3.1 summarizes the main electrical parameters of the reference AC cabinet. These parameters describe the nominal operating conditions of the system.

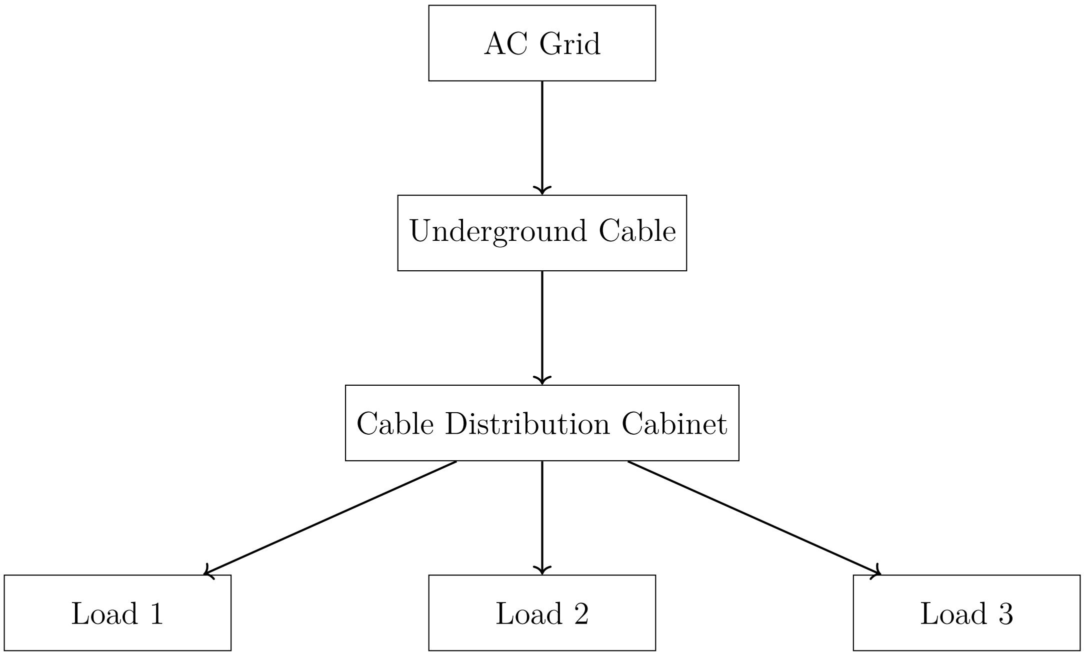

Figure 3.3: Architecture of the low-voltage distribution system.

Table 3.1: Electrical Ratings

Parameter	**Value**
Rated operating voltage (U_e)	400 V AC (line-to-line)
Rated insulation voltage (U_i)	1000 V
Frequency (f)	50 Hz
Rated current	1600 A
Number of poles	4P
Power factor ($\cos\varphi$)	0.9

These specifications show the electrical limits of the cabinet, and are used as reference values for the system in this study.

Busbar Supports

In this cabinet the KSST 316/23 busbar supports is used to mechanically hold and position the busbars inside the AC cabinet.
The busbar support technical data are summarized in Table 3.2 [24].

Table 3.2: Busbar Support Data

Parameter	Value
Device type	Busbar support
Suitable busbar ratings	400 A, 630 A, 1000 A, 1600 A
Number of poles	3P
Distance between phases	85 mm
Product net width	320 mm
Product net height	20 mm
Product net depth / length	60 mm
Product net weight	0.8 kg

Busbar System

This cabinet uses KSFS 1698 aluminum busbars. The main characteristics of the busbar system are summarized in Table 3.3.

Table 3.3: Busbar Ratings

Parameter	Value
Busbar material	Aluminum
Cross-sectional area (per phase)	1097.89 mm^2
Busbar length used in cabinet	950 mm
Rated current	1600 A
Rated insulation voltage (U_i)	1000 V
Protection class	IP2X °C

This busbar is designed for system rated up to 1000V AC, but in this cabinet they operate at 400 V AC and 1600 A rated current. The busbar system is designed with IP2X protection, which prevents accidental contact with live conductive parts. This means that the live parts are not directly accessible to touch [21].

Neutral / Protective Earth Busbar

This cabinet uses KSNS 1098 busbar as the neutral and protective earth conductor in the cabinet. The main characteristics of this busbar are summarized in Table 3.4.

Table 3.4: Neutral / Earth Busbar Ratings

Parameter	**Value**
Busbar type	KSNS 1098
Busbar material	Aluminum
Busbar length	950 mm
Rated current (thermal)	1000 A
Rated insulation voltage (U_i)	1000 V
Degree of protection	IP00

The KSNS 1098 busbar is used as the neutral and protective earth conductor in the cabinet. This busbar is designed for PEN, PE and N in low-voltage distribution systems. It provides a conventional thermal current capacity of 1000 A.

Fuse Switch Disconnectors

This cabinet uses SLE 2 fuse switch disconnectors for protection and switching of the outgoing feeder circuits. The main electrical ratings of the device are summarized in Table 3.5.

Table 3.5: Fuse Switch Disconnector Ratings (SLE2)

Parameter	**Value**
Device type	SLE 2 fuse switch disconnector
Number of poles	3P
Fuse type	NH
Fuse size	2
Material	Copper
Rated operational voltage	400 V AC
Rated insulation voltage (U_i)	1000 V
Rated impulse withstand voltage (U_{imp})	12 kV
Equivalent resistance with IFÖ NH2 gG 400A fuse	0.744 mΩ
Equivalent resistance without fuse	0.098 mΩ
Rated operational current	400 A
Rated conditional short-circuit current	50 kA
Cable cross-section	50 – 300 mm^2
Degree of protection	IP2X

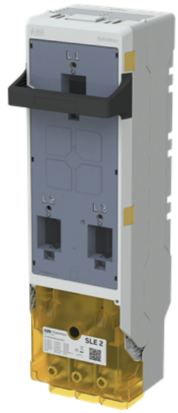

The SLE 2 fuse switch disconnector is mounted directly on the busbar system and is used to protect and disconnect the outgoing feeder cables. This fuse switch disconnector is designed to handle currents up to 400 A and is suitable for more demanding outgoing where higher power level is needed [19].

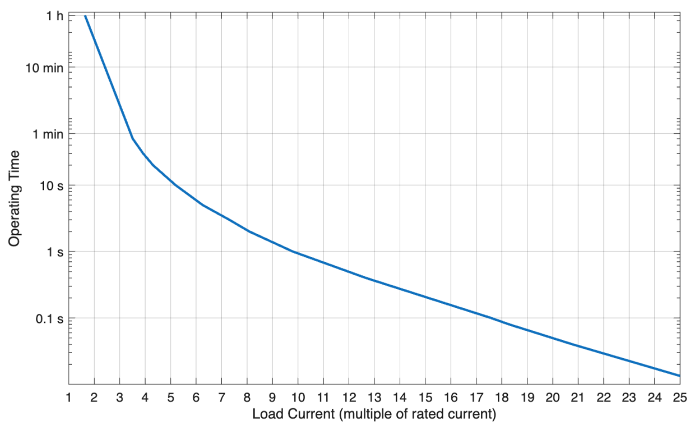

Figure 3.4: Time–current characteristic of IFÖ NH2 gG 400A fuse

In Figure 3.4, the operating behavior of a 400 A fuse is shown based on the time–current characteristic. This characteristic shows the relationship between the current passing through the fuse and its operating time for interrupting the current [34].

As the current increases, the operating time of the fuse decreases. For example, at a current of about 1.6 times the rated current, the operating time is around one hour, and with further increase in current, the operating time decreases rapidly. As can be seen in the time–current characteristic, at five times the rated current, the interruption time is in the range of a few seconds, and at much higher currents, the interruption operates in the order of hundredths of a second.

Cable Connection Interface

This cabinet uses ADI 300 insulated cable connectors for connection between incoming cables and the busbar system. The main electrical ratings of the connector are summarized in Table 3.6.

Table 3.6: Cable Connector Ratings

Parameter	**Value**
Connector type	ADI 300 insulated connector
Material	Aluminum
Cable cross-section	50 – 300 mm^2 (Al/Cu)
Rated operational voltage	1000 V
Rated insulation voltage (U_i)	1000 V
Rated impulse withstand voltage (U_{imp})	12 kV
Rated insulation current (I_i)	630 A
Degree of protection	IP2X
Standard	IEC 61238-1-1

The ADI 300 connector is used as the interface between the incoming cables and the phase busbars of the cabinet. The ADI 300 can be connected with cross-sectional areas ranging from 50 mm^2 to 300 mm^2. The connector provides IP2X protection from accidental contact and ensures a reliable connection to the busbar system [22].

Mechanical and Installation Characteristics

The mechanical and installation characteristics of the reference AC cabinet are summarized in Table 3.7 including the physical structure, installation conditions, and the environmental protection of the cabinet.

Table 3.7: Mechanical and Installation Characteristics

Parameter	**Value**
Installation type	Ground-mounted outdoor cabinet
Enclosure material	Galvanized steel
Degree of protection (enclosure)	IP34D
Dimensions (H × W × D)	889 mm × 996 mm × 312 mm
Weight	65 kg
Cooling principle	Natural ventilation

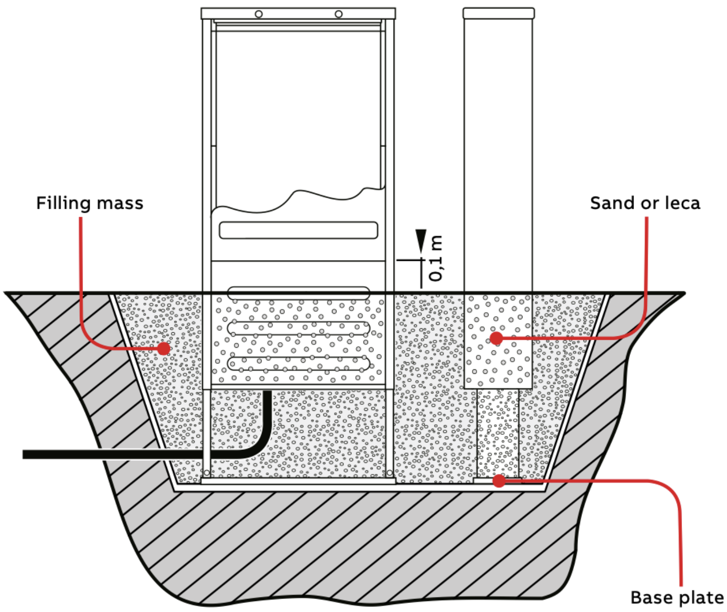

Figure 3.5: Installation combinations of Kabeldon enclosures [15]

Figure 3.6.shows the typical installation setup of the Kabeldon distribution cabinet. The cabinet is installed as a ground-mounted outdoor unit and is placed in the ground by base plate and filling material to provide mechanical stability.

Short-Circuit Performance

The short-circuit capability of the cabinet and the busbar system is summarized in Table 3.8.

Table 3.8: Short-Circuit Ratings

Parameter	**Value**
Short-time withstand current (I_{RSM})	30 kA (1 s)
Peak withstand current (I_{pk})	67 kA
Rated conditional short-circuit current (I_{cc})	3×315 A fuse

These values show the thermal and mechanical limits that the cabinet and busbar system can resist during short-circuit conditions.

3.2 DC Alternative Configuration (±380 V DC + N)

In this study, a bipolar three-wire DC system (±DC with neutral) with a voltage of ±380 V and a rated current os 1600 A is selected as the alternative distribution system.

The bipolar DC structure can support different load levels and connection types with the same distribution cabinet. between the positive and negative poles high power loads can be connected (760 V), and lower power loads can be connected between one pole and the neutral conductor (380 V). The bipolar structure also keeps the voltage balanced in the system and increases the flexibility of the network when supplying different types of loads.

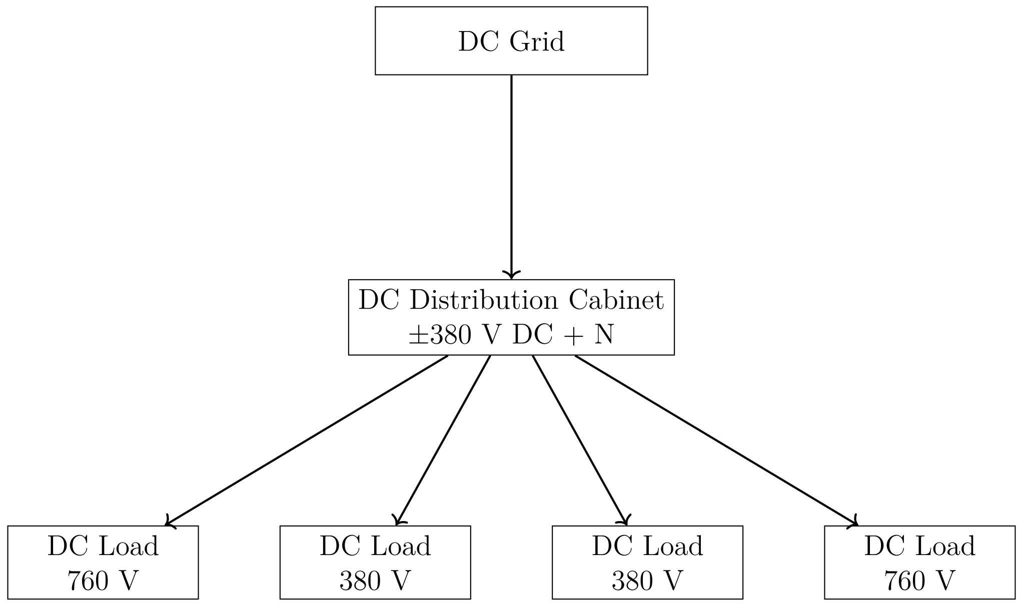

Figure 3.6: Conceptual DC distribution system supplying loads through the DC cabinet.

Figure 3.6 shows the structure of the proposed DC distribution system. When power is supplied from the DC grid, the cabinet is located between the DC grid and the loads as the distribution node, and then distributes power to different DC loads.

Electrical System

The electrical parameters of the proposed DC distribution system are summarized in Table 3.9.

Table 3.9: DC Electrical Ratings

Parameter	Value
System type	Bipolar DC (±380 V + N)
Rated current	1600 A
Rated operating voltage (U_e)	±380 V DC
Pole-to-pole voltage	760 V DC
Pole-to-neutral voltage	380 V DC
Rated insulation voltage (U_i)	1500 V
Number of poles	3 (N, −, +)

The DC system is a bipolar voltage of ±380 V with a neutral conductor, which gives a pole-to-pole voltage of 760 V and a rated current of 1600 A, which shows the current capacity of the system.

Busbar System

The DC cabinet uses the same KSFS 1673 aluminum busbar system as the reference AC cabinet. The same neutral busbar as in the reference AC cabinet is used. The electrical characteristics of the DC busbar system are summarized in Table 3.10.

Table 3.10: Busbar Ratings

Parameter	Value
Busbar material	Aluminum
Cross-sectional area (per phase)	1097.89 mm^2
Busbar length used in cabinet	950 mm
Rated current	1600 A
Rated operational voltage	760 V DC
Rated insulation voltage (U_i)	1000 V
Number of active current conductors	2 (+, −)
Protection class	IP2X
°C	

The system uses two active conductors (positive and negative) and one neutral conductor.

OTDC Switch-Disconnector

The OTDC switch-disconnector is a possible option for use in the DC cabinet. This switch is designed for direct current applications and can be used for switching, disconnection, and isolation of DC circuits. ABB has introduced this product for applications such as solar systems, energy storage systems, electric vehicle chargers, marine applications, DC microgrids, DC data centers, railway applications, and DC distribution systems. The main role of this switch will be to disconnect and isolate the outgoing DC feeders during operation, maintenance, and service[44].

The electrical characteristics of the the OTDC switch-disconnector are summarized in Table 3.11.

Table 3.11: Switch-disconnector

Parameter	Value
Device type	OTDC switch-disconnector
Application	Switching and isolation of DC feeders
Rated current range	16–1600 A
System voltage in this thesis	760 V DC
Main function	Disconnecting and isolating feeders
Use in proposed cabinet	Outgoing DC feeder switching

Mechanical and Installation

The DC cabinet has the same mechanical and installation characteristics as the AC distribution cabinet. This is because the DC cabinet is based on the same physical enclosure and structural design as the AC cabinet. The installation concept shown in Figure 3.6 is applicable to the DC cabinet.

The mechanical and installation parameters of the DC cabinet are summarized in Table 3.12.

Table 3.12: DC Mechanical and Installation

Parameter	Value
Installation type	Ground-mounted outdoor cabinet
Enclosure material	Galvanized steel
Degree of protection (enclosure)	IP34D
Dimensions (H × W × D)	889 mm × 996 mm × 312 mm
Weight	65 kg
Cooling principle	Natural ventilation
Standard compliance	IEC 61439

The cabinet is installed outdoors on the ground and fixed in place with base plate and filling material to provide mechanical stability.

4

AC Cabinet Analysis

4.1 Electrical Characteristics of the AC Cabinet

In this chapter, the AC cabinet is analyzed. The purpose of this analysis is to evaluate the main characteristics of the cabinet during normal operation. This cabinet operates as a three-phase low-voltage AC system which has 400 V voltage line-to-line and 1600 A rated current. The system is assumed to operate under steady-state conditions. So, the power of this system can be calculated as

$$P_{AC} = \sqrt{3} V_{LL} I \cos\phi \tag{4.1}$$

$$V_{LL} = 400\,V$$

$$I = 1600\,A$$

$$\cos\phi = 0.9$$

where V_{LL} is the line-to-line voltage, I is the rated current, and $\cos\phi$ is the power factor. So, the transmitted active power is

$$P \approx 998\,kW$$

when the system is balanced, all three phases have the same voltage, current, and power.

The current per phase is

$$I_{L1} = I_{L2} = I_{L3} = 1600 \text{ A}$$

The voltage per phase is

$$V_{\text{phase}} = \frac{V_{LL}}{\sqrt{3}} \approx 230 \text{ V}$$

The power per phase is

$$P_{\text{phase}} = \frac{P_{\text{total}}}{3} \approx 333 \text{ kW}$$

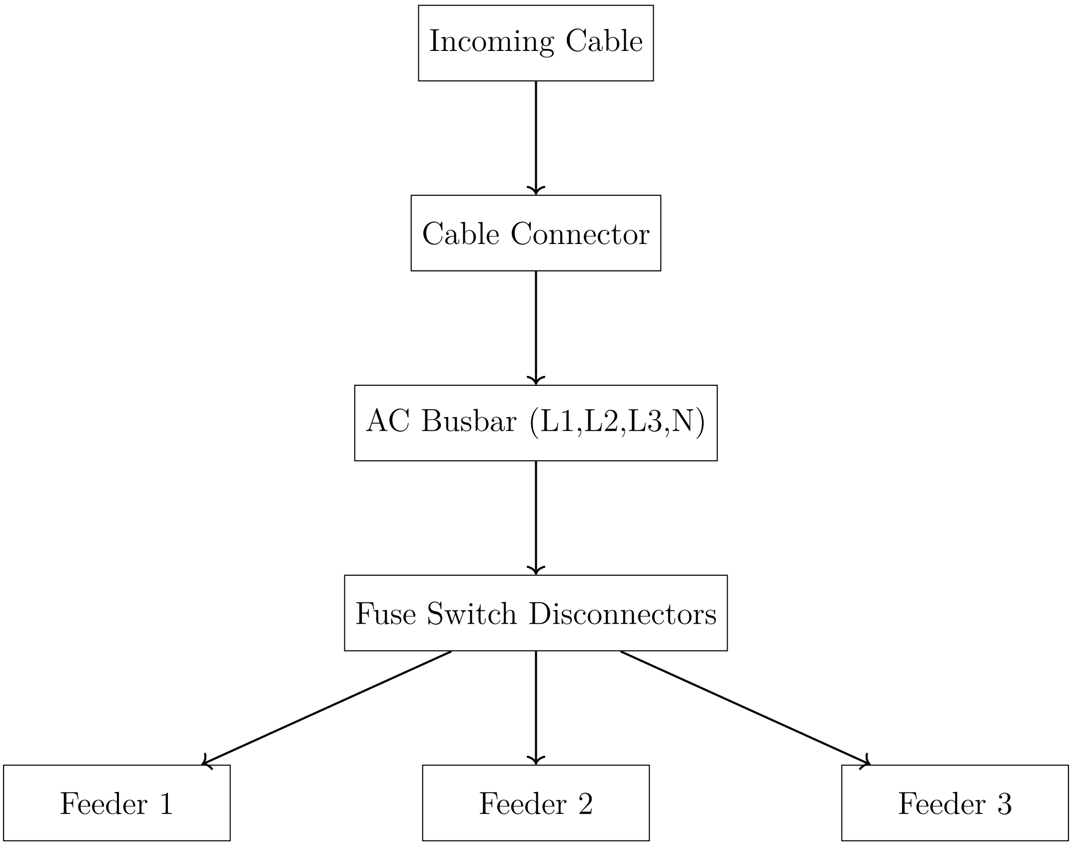

Figure 4.1: The internal parts of the AC distribution cabinet.

This AC distribution cabinet is designed to handle a power level close to $1MW$ under rated operating conditions. In this cabinet, the busbar is the main part that carries the current and it distributes the power from the incoming sours to the outgoing feeders. [12, 13].

4.2 AC Power Loss conduction

In an AC distribution system, the main reason for power losses is the electrical resistance of the conductors and electromagnetic phenomena. An AC system operates with alternating current and a specific frequency, which leads to more effects in the conductors. The main effects are reactive power, power factor, and skin effect.

Reactive power and a low power factor increase the current flow without transferring useful power. The skin effect is caused by the frequency, it makes the current flow closer to the surface of the conductor, which increases the resistance of the conductor which leads to more losses.

Under steady-state operating conditions, each phase has the same current therefore, the total conduction losses can be calculated by summing the losses in the three phase conductors. during balanced operating conditions, the current in the neutral conductor is very low and can be neglected [5].

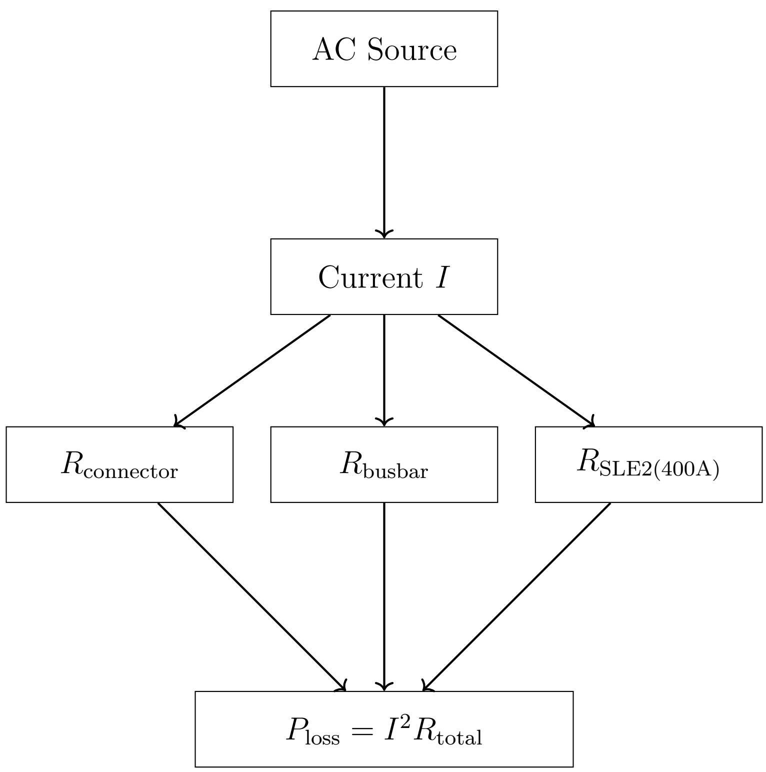

Figure 4.2: Electrical loss model in the AC cabinet.

The power loss of each component calculated as

$$P = I^2 R$$

where P is the power loss, I is the operating current, and R is the electrical resistance.

Cable connector losses

The resistance of one cable connector is

$$R_{\text{connector}} = 4.2 \times 10^{-6}\ \Omega$$

$$I = 300\ \text{A}$$

The power loss of each connector becomes

$$P_{\text{connector},1} = 0.378\ \text{W}$$

$$P_{\text{connector,total}} = 3 \times 0.378 = 1.134\ \text{W}$$

Busbar losses

The AC cabinet has three busbars, the resistance of one busbar is

$$R_{\text{busbar}} = 2.44 \times 10^{-5}\ \Omega$$

$$I = 300\ \text{A}$$

The power loss for each busbar becomes

$$P_{\text{busbar},1} = 2.196\ \text{W}$$

$$P_{\text{busbar,total}} = 3 \times 2.196 = 6.588\ \text{W}$$

SLE 2 fuse switch disconnector losses

The SLE 2 fuse switch disconnector resistance is

$$R_{\text{SLE2}} = 0.744\ \text{m}\Omega$$

$$I = 300\ \text{A}$$

The power loss of the SLE 2 switch disconnector is

$$P_{\text{SLE2}} = I^2 R$$

$$P_{\text{SLE2}} = (300)^2 \times 0.000744 = 66.96\ \text{W}$$

Total power loss

The total power loss inside the AC cabinet is

$$P_{\text{total}} = P_{\text{busbar,total}} + P_{\text{connector}} + P_{\text{SLE2}}$$

$$P_{\text{total}} = 74.68 \text{ W}$$

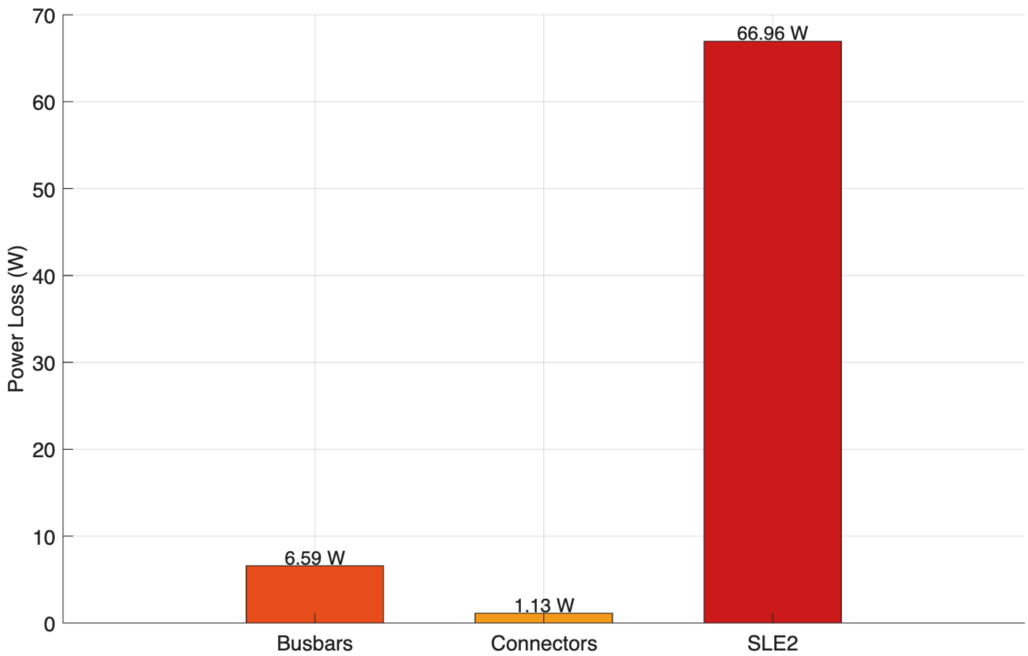

Figure 4.3: Power losses in the components of the AC cabinet at 300A

The total power loss in this cabinet is 74.68 W. As shown in the figure 4.3, the SLE2 has the highest losses, which is 66.96 W, the busbars have losses of 6.59 W, and the connectors have losses of 1.13 W. Since the losses are due to the current flow and the power factor, If these parameters change, the losses also change. Higher current leads to higher losses, and a lower power factor also leads to higher losses [12].

Temperature effect on total power loss

In addition, the resistance of the system changes with temperature. The resistance calculated before was for a temperature of 20°C.

To calculate the resistance value of the the conductors, the standard temperature correction equation can be written as [26, 27].

$$R(T) = R_{20}\left[1 + \alpha(T - 20)\right]$$

where R_{20} is the resistance at 20°C, T is the temperature of the conductor and α is the temperature coefficient of the conductor material.

with this equation, the resistance of the system can be estimated at different temperatures. In winter in Sweden at a temperature of -20°C.

For the aluminum parts (busbar and cable connector), the temperature coefficient is

$$\alpha_{\mathrm{Al}} = 0.00403\ /^{\circ}\mathrm{C}$$

$$R_{\mathrm{Al}}(-20) = R_{20}[1 + 0.00403(-20 - 20)]$$

$$R_{\mathrm{Al}}(-20) = R_{20}(0.8388)$$

The result becomes

$$R_{\mathrm{busbar},-20} \approx 2.04 \times 10^{-5}\ \Omega$$

$$R_{\mathrm{connector},-20} \approx 3.52 \times 10^{-6}\ \Omega$$

For the copper parts (SLE 2 fuse switch), is

$$\alpha_{\mathrm{Cu}} = 0.00393\ /^{\circ}\mathrm{C}$$

$$R_{\mathrm{Cu}}(-20) = R_{20}[1 + 0.00393(-20 - 20)]$$

$$R_{\mathrm{Cu}}(-20) = R_{20}(0.8428)$$

$$R_{\mathrm{SLE2},-20} = 6.27 \times 10^{-4}\ \Omega$$

Then the total power loss of the system in winter becomes

$$P_{loss,total} \approx 62.62\,W$$

In summer at temperature of 30°C

$$R_{total}(30^{\circ}C) = 8.62 \times 10^{-4}\ \Omega$$

Then the total power loss in the busbar in summer when the ambient temperature is 30°C becomes

$$P_{loss,total} \approx 77.56\,W$$

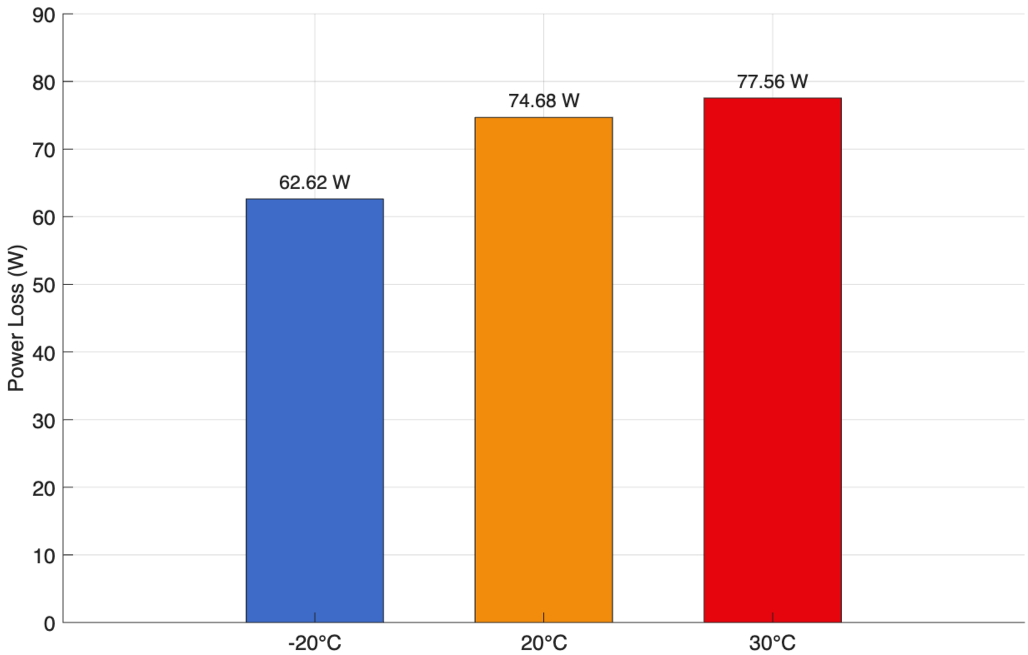

Figure 4.4: AC cabinet power loss at different ambient temperatures at 300 A

The results show in Figure 4.4, that the ambient temperature has a direct impact on the power losses of the system. At a temperature of 20°C, the total power loss was 74.68 W. When the ambient temperature reaches 30°C in summer, the total losses increase to around 77.56 W, in winter, when the ambient temperature decreases to −20°C, the power losses decrease to 62.62 W.

This result shows that higher ambient temperatures lead to higher electrical resistance in the components, which leads to higher conduction losses of the system, and this shows that from a summer condition of 30°C to a winter condition of −20°C, the difference in the system losses is approximately 14.94 W.

4.3 Thermal Performance of the AC Cabinet

In this section, the thermal behavior of the AC cabinet is analyzed. In this cabinet, the temperature rise inside the cabinet is evaluated based on the power losses of the system. This means that the losses in different components of the system lead to higher temperature inside the cabinet.

In this cabinet the Busbars and the Fuse Switch Disconnectors are the main sources of heat generation. When electrical current flows through these components, due to their resistance, losses are generated and these losses are released as heat. Therefore, electrical losses are considered as the main source of heat generation in this cabinet.

This cabinet is installed outdoors and no forced cooling system such as a fan is used, the cooling process is through natural air ventilation. Heat is transferred through the air inside the cabinet to the cabinet body, from the cabinet surface to the ambient air, and a part of this heat also be transferred to the ground [16].

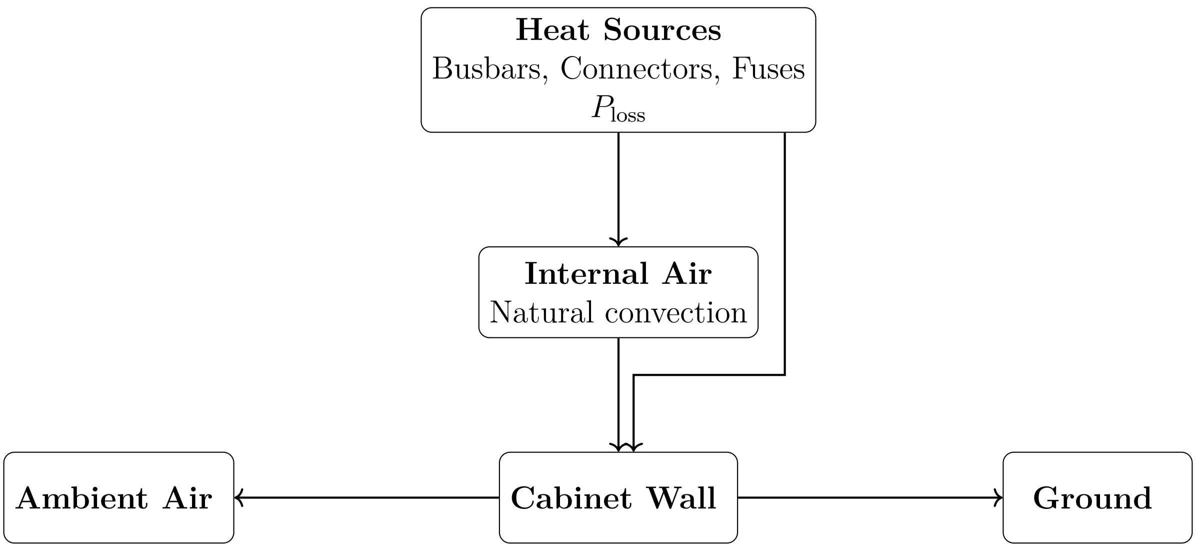

Figure 4.5: Heat flow inside the AC cabinet

The calculation of the temperature of this cabinet is based on IEC TR 60890 standard, which provides a practical and empirically validated method to estimate the temperature rise of ABB cabinets [29].

According to this standard, the internal air temperature can be determined as

$$T_{\text{inside}} = T_{\text{ambient}} + \Delta T$$

where ΔT is the temperature rise inside the cabinet due to the total power losses.

The main steps of the calculation in this method are as

- Determination of the effective cooling surface of the enclosure
- identifying the type of enclosure and its installation conditions
- Calculation the temperature rise at the mid-height of the cabinet
- Calculation the temperature rise at the top of the cabinet, where the hottest part of the cabinet is

Effective Cooling Surface

The effective cooling surface A_e is the area that heat is dissipation. This can be calculate as

$$A_e = \sum(A_o \times b)$$

where A_o is the cabinet surface area and b is the surface factor. The surface factor represents how much each part of the cabinet contributes to heat dissipation.

- Top surface (exposed): $b = 1.4$
- Side surfaces (exposed): $b = 0.9$
- Bottom surface: 0

The dimensions of the cabinet are

$$H = 0.889 \text{ m}, \quad W = 0.996 \text{ m}, \quad D = 0.312 \text{ m}$$

The calculated effective cooling surface is:

$$A_e \approx 2.528\,\text{m}^2$$

Temperature Rise at Mid-Height

For this type of cabinet without forced ventilation, To obtain the temperature at the middle of the cabinet, it can be calculated as [29]

$$\Delta t_{0.5} = k \cdot d \cdot P^x$$

where P is the total power loss, k is a coefficient depending on A_e, d is a correction factor related to internal partitions and x is an empirical exponent.

The power losses are from the busbars, cable connectors, and the SLE2 fuse switch. When the current in the busbars and cable connectors is 300 A and the current in the SLE2 is 300 A, the losses of each part are

$$P_{\text{busbars}} = 6.59 \text{ W}$$

$$P_{\text{connectors}} = 1.13 \text{ W}$$

$$P_{\text{SLE2}} = 66.96 \text{ W}$$

$$P_{\text{total}} = 74.68 \text{ W}$$

From IEC TR 60890, the coefficient k is calculated as

$$k = 0.58 \times (A_e)^{-0.795}$$

$$k \approx 0.277$$

Since no horizontal partitions are considered

$$d = 1.0$$

The exponent is

$$x = 0.804$$

The temperature rise at the middle of the cabinet can be calculated as

$$\Delta t_{0.5} = k \cdot d \cdot P^x$$

Substituting the values:

$$\Delta t_{0.5} = 0.277 \times 1.0 \times (74.68)^{0.804}$$

$$\Delta t_{0.5} \approx 8.86°C$$

In this cabinet, the temperature at the middle of the cabinet increases 8.86°C above the ambient temperature.

Temperature Rise at the Top of the Cabinet

The temperature at the top of the cabinet is higher, and this is what we expect since in a closed environment the temperature at the top is higher than at the bottom. It calculate as

$$\Delta t_{1.0} = c \cdot \Delta t_{0.5}$$

The coefficient c depends on the enclosure geometry and is obtained using the height/base factor

$$f = \frac{h^{1.35}}{A_b}$$

$$A_b = W \times D$$

The calculated value is

$$f \approx 2.745$$

Using IEC TR 60890 , the coefficient c is

$$c = -0.0017f^2 + 0.055f + 1.182$$

$$c \approx 1.32$$

$$\Delta t_{1.0} \approx 11.70°C$$

The temperature at the top of the cabinet, as we can see, becomes 11.70°C higher than the ambient temperature.

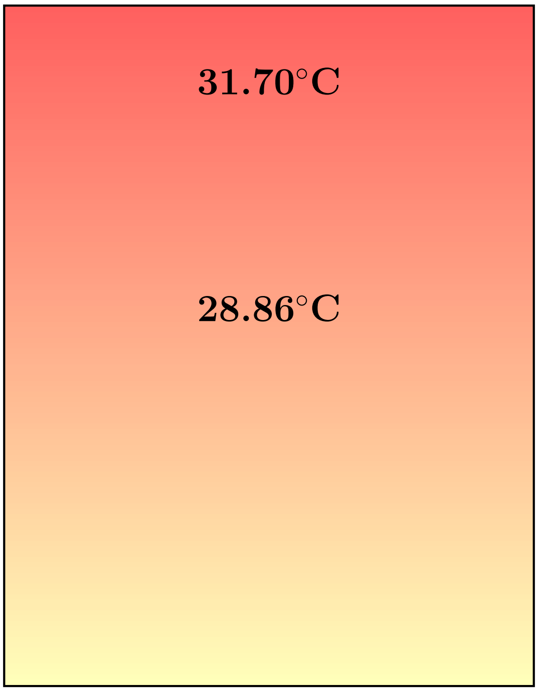

If the ambient temperature is 20°C, the temperature at the middle of the cabinet becomes 28.86°C, and the temperature at the top of the cabinet near the roof becomes 31.70°C.

Temperature effect

In fact, the season and the ambient temperature have a direct effect on the thermal behavior of the cabinet.

As calculated in the previous sections, the resistance of the conductors becomes lower in winter, then the power losses in winter are also lower than summer.

Winter condition

- Ambient temperature: $T_{\text{amb}} = -20°\text{C}$
- System resistance: $R(-20°C) = 6.96 \times 10^{-4}\ \Omega$
- Total power loss: $P_{\text{loss}} = 62.62\ \text{W}$

The temperature rise generated inside the cabinet due to system losses become

$$\Delta T_{\text{middle}} = 7.69°\text{C}$$
$$\Delta T_{\text{top}} = 10.15°\text{C}$$

The final temperature under winter conditions with an ambient temperature of $-20°$C, become

$$T_{\text{middle}} = -12.31°\text{C}$$
$$T_{\text{top}} = -9.85°\text{C}$$

Summer Condition

- Ambient temperature: $T_{\text{amb}} = 30°\text{C}$
- System resistance: $R_{\text{total}} = 8.62 \times 10^{-4}\ \Omega$
- Total power loss: $P_{\text{loss}} = 77.56\ \text{W}$

The temperature rise generated inside the cabinet due to system losses become

$$\Delta T_{\text{middle}} = 9.13°\text{C}$$
$$\Delta T_{\text{top}} = 12.05°\text{C}$$

The final temperature under summer conditions with an ambient temperature of 30°C, become

$$T_{\text{middle}} = 39.13°\text{C}$$
$$T_{\text{top}} = 42.05°\text{C}$$

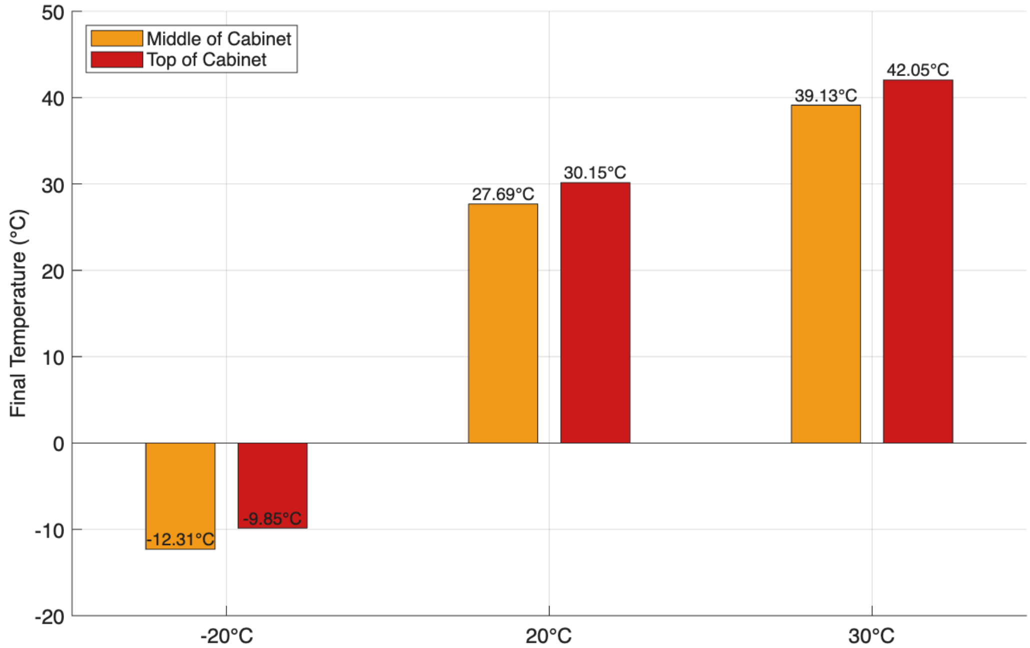

Figure 4.6: AC cabinet temperatures at 300A under different ambient conditions

As shown in Fig. 4.6, the temperature inside the cabinet in winter is between −12.31°C and −9.85°C. While in summer, the temperature inside this cabinet is between 39.13°C and 42.05°C.

This temperature difference is due to the direct effect of ambient temperature and the system losses. As we calculated in the previous sections, in summer when the ambient temperature increases, this leads to higher resistance in the conductors and therefore more heat generation. On the other hand, in winter when the ambient temperature is lower, the resistance of the system decreases and the generated heat is also lower. As a result, this behavior is completely expected.

This result shows that the electrical operating conditions of the system have a direct effect on the thermal behavior of the cabinet. Parameters such as ambient temperature, current level, resistance of the conductors, and generated power losses play an important role in the thermal behavior of the system. So, these factors must be considered when designing a distribution cabinet [16, 17].

Temperature Estimation of Internal Components

After determining the internal temperature of the cabinet using the IEC TR 60890, the next step is to calculate the temperature of the components inside the cabinet. In the IEC method, the standard provides the internal air temperature of the cabinet, but it does not directly give the temperature of specific components such as busbars, connectors, and fuse switch disconnectors.

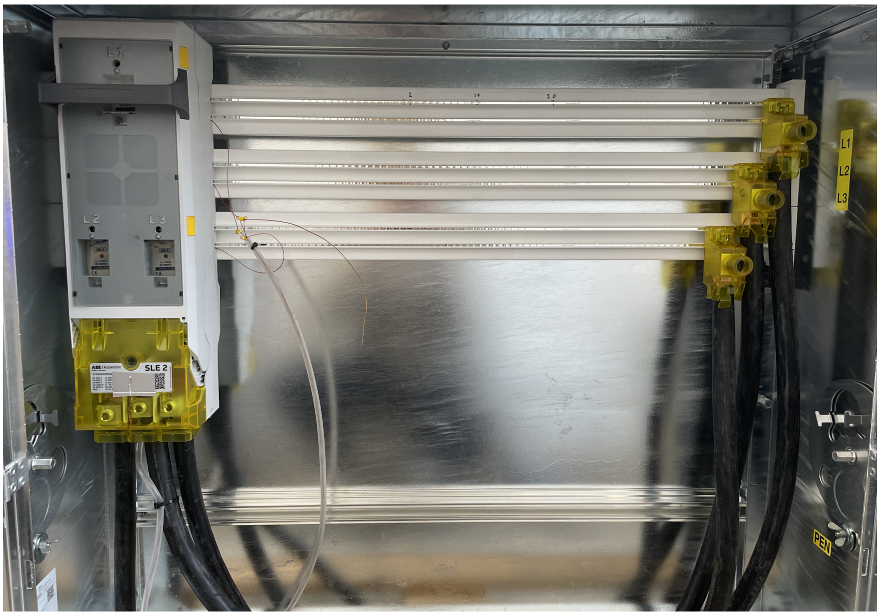

Figure 4.7: AC Cabinet Components

The figure shows the inside of the AC cabinet. As shown in figure 4.7 , the cable connectors are located on the right side of the cabinet, where the incoming cable is connected. The busbars are placed inside the cabinet and carry the current transfer path. On the left side of the cabinet, the SLE2 fuse switch is installed, which is responsible for protection and power distribution. The outgoing cables toward the load also exit from this part. In this cabinet, the power enters from the right side, then it transferrer through the busbars toward the fuse, and then exits toward the load.

A lumped thermal model is used to estimate the temperature rise of each component inside the cabinet. The heat generated by each component is equal to its electrical power loss, and this heat is transferred to the internal air of the cabinet.

The heat transfer equation is

$$Q = hA(T_s - T_\infty)$$

where Q is the heat flow (W), h is the heat transfer coefficient (W/m^2K), A is the surface area (m^2), T_s is the surface temperature, and T_∞ is the ambient temperature.

For natural air convection, the heat transfer factor is between 5 and 20 W/m^{2}K. In this analysis, I assumed $h = 8\,\mathrm{W/m^2K}$ since the cabinet is cooled by natural convection without forced ventilation or fan [14].

$$h = 8\,W/m^2K$$

$$T_{amb} = 20°C$$

$$Q \approx P_{loss}$$

Busbars

The busbars are one of the main heat generating components in the cabinet. So, the electrical power loss at a current of 1600 A, in each phase is

$$P_{\text{loss busbar}} = 62.46\,W$$

$$P_{\text{total loss busbar}} = 187.38 \text{ W}$$

The busbar surface area is

$$t_{\text{eq}} = \frac{A}{W} = \frac{1096}{65} \approx 16.86 \text{ mm}$$

$$A_{\text{busbar}} = 2(LW + Lt + Wt) = 0.1577 \text{ m}^2$$

$$\Delta T_{\text{busbar}} = \frac{P_{\text{busbar}}}{hA_{\text{busbar}}} \approx 49.5°C$$

The heat generated in each busbar corresponds to a temperature increase of 49.5°C. As we can see in Figure 4.7, busbar L1 is located at the top of the cabinet, temperature at the top of the cabinet, is 59.6°C. it expected that the final temperature of busbar L1 becomes approximately 109.1°C.

Since bus bar L3 is located approximately in the middle of the cabinet and the temperature is 50°C, the temperature of L3 is expected to be 99.5°C. Due to this result, busbar L1 can be the hottest busbar and the hottest point in this cabinet.

Cable Connectors

The power losses for the cable connectors at a current of 630 A, based on their resistance is

$$P_{\text{connector}} = 1.67 \text{ W}$$

The connector surface area is

$$A_{\text{connector}} = 2(HW + HD + WD) = 0.03373 \text{ m}^2$$

The temperature rise of the connector is

$$\Delta T_{\text{connector}} = \frac{P_{\text{connector}}}{hA_{\text{connector}}} \approx 6.18°C$$

In the cable connectors, similar to the busbars it is also expected that the temperature in connector L1 is higher than in connector L3, exactly due to their position in the cabinet.

SLE 2

The power loss of the SLE 2 switch disconnector at a current of 400 A, based on its resistance, is

$$P_{\text{SLE2}} = 119.04 \text{ W}$$

The surface area of the SLE 2 is

$$A_{\text{SLE2}} = 2(HW + HD + WD) = 0.3979 \text{ m}^2$$

The temperature rise of the SLE 2 is

$$\Delta T_{\text{SLE2}} = \frac{P_{\text{SLE2}}}{hA_{\text{SLE2}}} \approx 37.3°C$$

In the SLE2 fuse switch, the temperature rise is 37.3°C. As shown in figure 4.7, due to the dimensions and the position of this fuse switch in the cabinet, where part of it is located in the upper region of the cabinet and another part is in the middle region. This leads to the expectation that the temperature at the upper part of the fuse is higher than the lower part.

4.4 Efficiency of the AC Cabinet

The efficiency of this AC cabinet can be evaluated based on the transmitted power and the total power losses in the system.

The efficient of the system can be calculate bay

$$\eta = \frac{P_{out}}{P_{out} + P_{loss}} \tag{4.2}$$

For this cabinet, the transmitted power based on the operating voltage of 400 V, current of 300 A, and power factor of 0.9 is 187.06KW and the total conduction losses in the Ac cabinet were 74.68W. The efficiency of this cabinet is 99.96%. This means that the losses are approximately 0.04%. At part loading, When the operating current becomes lower, the cabinet losses also become lower. This is because conduction losses depend on the square of the current.

Efficiency is evaluated by comparing the input power and the output power of the system and it is directly related to the power losses in the system.

In practice, efficiency shows how much of the input power is delivered to the load and how much is lost inside the system. In this system, the losses are small compared to the transmitted power, so the cabinet efficiency is quite high.

4.5 Short-Circuit Current in the AC Cabinet

Short-circuit current in the AC cabinet occurs when a connection is created between phases or between phases and earth with very low impedance, meaning the resistance between them is very low, and this can happen as phase-to-phase or phase-to-earth. This causes the current to increase very rapidly and this current creates two main effects in the system, thermal stress and mechanical forces. These effects can have a big impact on the busbars and the structure inside the cabinet.

To analyze the short-circuit behavior in our AC cabinet. The short-circuit current of the system is considered based on the design specifications as

$$I_{sc} = 30 \text{ kA}$$

which represents the RMS value of the short-circuit current. Also, the instantaneous peak current is equal to

$$I_{peak} = 67 \text{ kA}$$

The RMS current represents the thermal effect of the current on the components of the system, and the peak current represents the maximum instantaneous mechanical force applied to the cabinet equipment.
These values are used to evaluate the thermal and mechanical effects of short circuits in the system [33].

The heat generated during a short circuit can be calculated as

$$Q = I^2 Rt$$

where Q is the generated thermal energy (J), I is the short-circuit current (A), R is the busbar resistance (Ω) and t is the duration of the short-circuit current (s)

$$Q = (30000)^2 \times 2.44 \times 10^{-5} \times 1$$

$$Q \approx 21.96 \text{ kJ}$$

$$\Delta T = \frac{Q}{mc}$$

where c is the specific heat capacity of the busbar, m is the mass of one busbar

$$\Delta T = \frac{21960}{2.82 \times 900}$$

$$\Delta T = \frac{21960}{2538}$$

$$\Delta T \approx 8.65°C$$

In this result, we can see that when a short circuit of 30 kA occurs in this cabinet, then a temperature rise of 8.65°C appears in the busbars.

The mechanical force during a hort-circuit current in this cabinet can be calculate as

$$\frac{F}{L} = \frac{\mu_0}{2\pi}\frac{I^2}{d}$$

where $\mu_0 = 4\pi \times 10^{-7}\,\mathrm{H/m}$, I is the peak short-circuit current, and d is the distance between the conductors.

$$d = 0.085\,\mathrm{m}$$

$$I = 67000\,\mathrm{A}.$$

$$\frac{F}{L} \approx 10562\,\mathrm{N/m}.$$

This means that the electromagnetic force between each busbars is approximately

$$10.6\,\mathrm{kN/m}.$$

This results show that mechanical stress during short circuit in this cabinet is very high. These forces can move the busbars from their position or bend them.

5

DC Cabinet Analysis

5.1 Electrical Characteristics of the DC Cabinet

The alternative DC system selected in this study is a bipolar three-wire DC system ($\pm$DC with neutral) operating at ± 380 V with one pole and neutral conductor and ± 760 V between each pole. The current is assumed to be 1600 A.

The bipolar structure allows flexible load connection while keeping the voltage balanced, and allows the system to support different load levels and connection types. Based on this parameters, the transmitted power of the system can be calculated as

$$P_{DC} = V_{DC} I \tag{5.1}$$

$$P \approx 1.216 \text{ MW}$$

The transmitted power of the DC system is approximately 1.22 MW, this means 608 KW per pole.

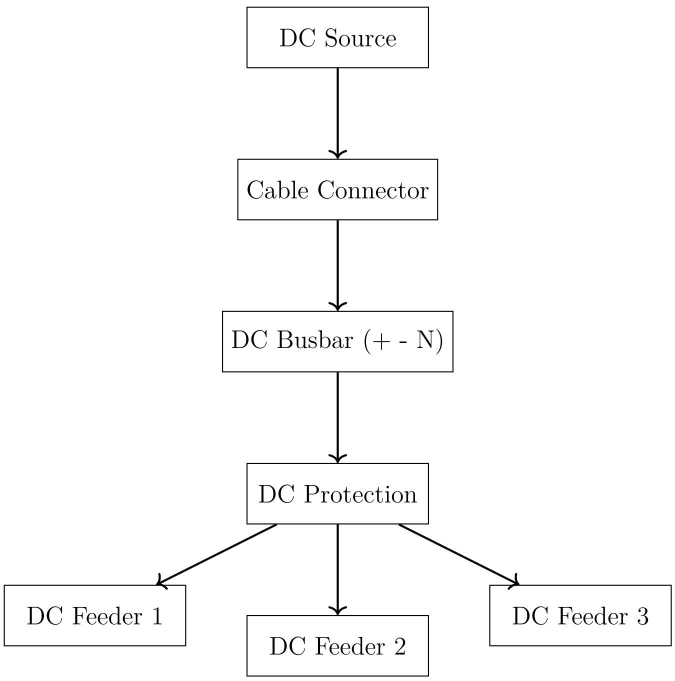

Figure 5.1: the structure of DC distribution cabinet

The DC system can transmit about 1.2 MW of power when both poles are used at a voltage of 760 V. The bipolar structure also allows the system to operate with one pole and the neutral conductor, which can provide approximately 600 kW of transmitted power. This means that the system has flexibility in power delivery while still providing power capability [1].

5.2 DC Power Loss conduction

In this analysis, a current of 1600 A is assumed as a hypothetical scenario to investigate the maximum possible power losses and the thermal behavior of the DC cabinet. Therefore, this current is considered a theoretical assumption for analysis purposes and does not represent an actual operating condition of the system.

In a DC distribution system, the main source of power losses is the electrical resistance of the conductors. In DC systems, the current flows in one direction and there is no operating frequency and other phenomena such as reactive power, power factor, and the skin effect. Because of that, the resistance of the conductors in a DC System is lower.

In this cabinet, the losses of the busbars and the cable connectors are calculated. The losses of other components such as DC-rated switch-disconnector are not considered, because because the final DC adaptering is not built and verified for installation in this system. So, we only calculate the losses of the busbars and cable connectors.

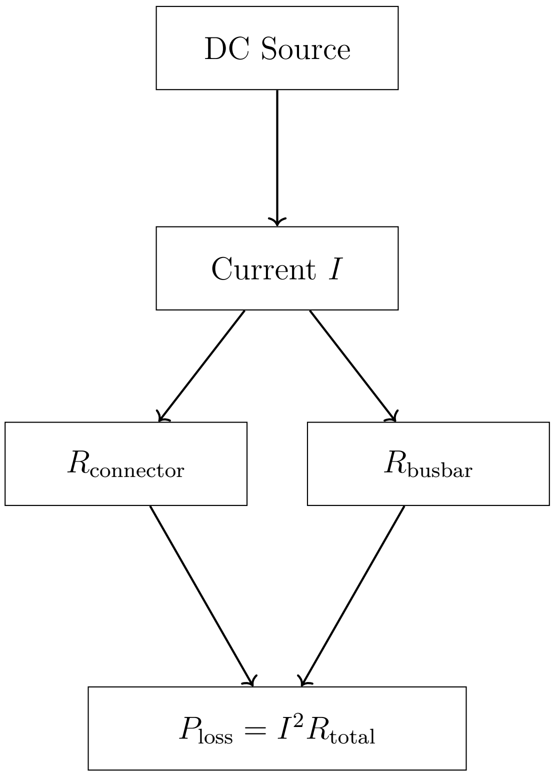

Figure 5.2: Electrical loss model in the DC cabinet.

The power losses in this cabinet can be calculated as

$$P_{loss} = I^2 R$$

Where I is the conductor current and R is the electrical resistance.

Cable connector losses

The resistance of one cable connector is

$$R_{\text{connector}} = 4.2 \times 10^{-6}\ \Omega$$

$$I = 1600\ \text{A}$$

The power loss of each connector becomes

$$P_{\text{connector,1}} = 10.75\ \text{W}$$

$$P_{\text{connector,total}} = 2 \times 10.75 = 21.5\ \text{W}$$

Busbar losses

The AC cabinet has three busbars, the resistance of one busbar is

$$R_{\text{busbar}} = 2.44 \times 10^{-5}\ \Omega$$

$$I = 1600\ \text{A}$$

The power loss for each busbar becomes

$$P_{\text{busbar,1}} = 62.46\ \text{W}$$

$$P_{\text{busbar,total}} = 2 \times 62.46 = 124.92\ \text{W}$$

Total power loss

The total power loss inside the DC cabinet is

$$P_{\text{total}} = P_{\text{busbar,total}} + P_{\text{connector}}$$

$$P_{\text{total}} = 146.42\ \text{W}$$

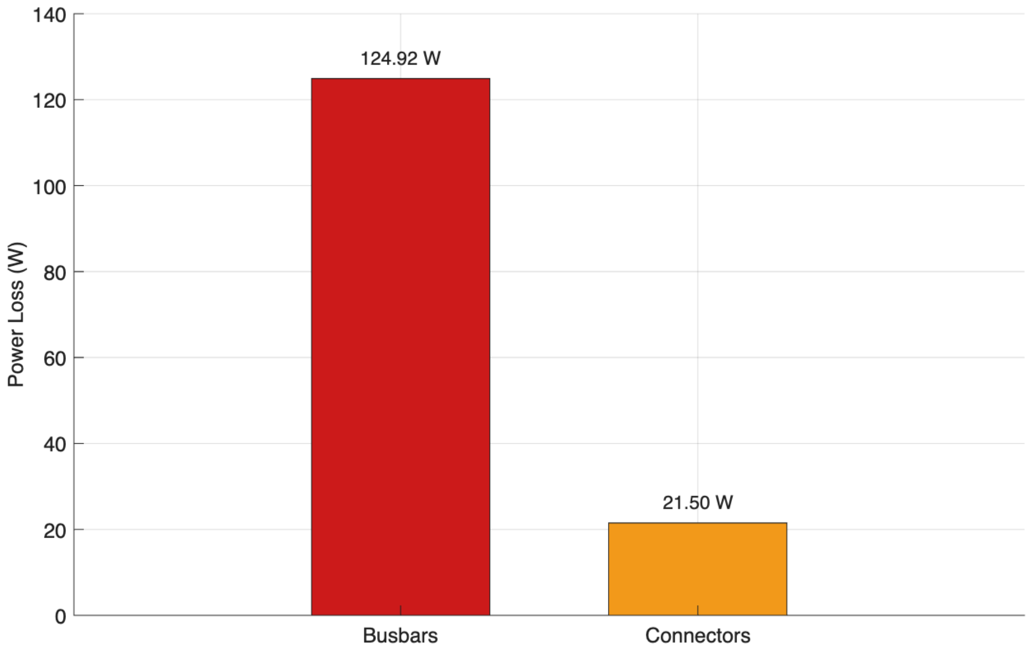

Figure 5.3: DC component power loss at 1600A

As shown in Figure 5.3 the busbar power Losses is 124 W and the connectors losses is 21 W in the DC cabinet. This result shows that the total conduction losses in the DC system are about 146 W, when this power loss is compared with the total power delivered by the system, it can be seen that the losses are relatively small. The main reason for this low loss is the DC structure, which leads to the busbar operating with high efficiency [12].

Temperature effect on total power loss

In fact, the resistance of the system is different in different seasons. In the previous calculations, the power losses were evaluated under normal conditions at an ambient temperature of 20°C. Now, I want to see how the system resistance and power losses change when the ambient temperature increases to 30°C in summer and decreases to −20°C in winter in Sweden.

To calculate the resistance value of the the conductors, the standard temperature correction equation can be written as [26, 27].

$$R(T) = R_{20}\left[1 + \alpha(T - 20)\right]$$

where R_{20} is the resistance at 20°C, T is the temperature of the conductor and α is the temperature coefficient of the conductor material.

At $20°C$, the total resistance of the DC cabinet is

$$R_{\text{total},20°C} = 5.72 \times 10^{-5}\ \Omega$$

At $30°C$

$$R_{\text{total},30°C} = 1.0403 \times R_{\text{total},20°C}$$

$$R_{\text{total},30°C} \approx 5.95 \times 10^{-5}\ \Omega$$

At $-20°C$

$$R_{\text{total},-20°C} = 0.8388 \times R_{\text{total},20°C}$$

$$R_{\text{total},-20°C} \approx 4.80 \times 10^{-5}\ \Omega$$

After determining the total resistance at each temperature, the power losses

At $30°C$

$$P_{30°C} = (1600)^2 \times 5.95 \times 10^{-5}$$

$$P_{30°C} \approx 152.3\ \text{W}$$

At $-20°C$:

$$P_{-20°C} = (1600)^2 \times 4.80 \times 10^{-5}$$

$$P_{-20°C} \approx 122.8\ \text{W}$$

The total power loss in the DC system at **30°C** becomes **152.3 W**.

The total power loss in the DC system at **20°C** becomes **146.4 W**.

The total power loss in the DC system in winter (**-20°C**) becomes **122.8 W**.

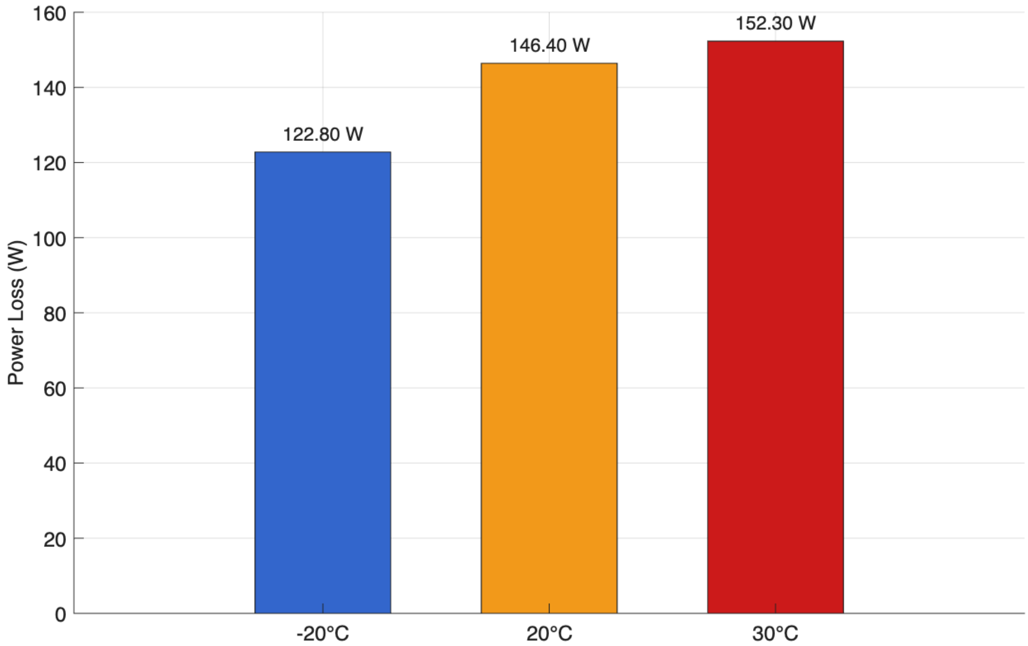

Figure 5.4: DC component power loss at different ambient temperatures at 1600A

In Figure 5.4, it can be seen that when the ambient temperature increases, the total resistance of the aluminum conductors increases, which leads to higher conduction losses and at lower temperatures, the resistance and power losses decrease.

This means that the ambient temperature has direct effects on the system power losses. As shown, when the temperature is 30°C, the system power loss is 152.3 W, and when the temperature becomes 20°C, the power loss becomes 146.4 W. When the temperature decreases to -20°C in winter, the power loss decreases to 122.8 W. So, due to the different ambient temperatures, the resistance of the conductors changes, which leads to a change in the power losses of the system.

5.3 Thermal Performance of the DC Cabinet

In a DC distribution system, most electrical losses are converted into heat in the conductors and busbars. The temperature rise of the cabinet is directly related to the internal power losses and the ambient temperature. Higher electrical losses generate more heat, which lead to higher temperature of the cabinet.

Since the cabinet is installed outdoors, the heat inside the cabinet transferred to the surrounding environment through natural convection. Therefore, the cabinet temperature depends on the power losses and the ambient temperature [25].

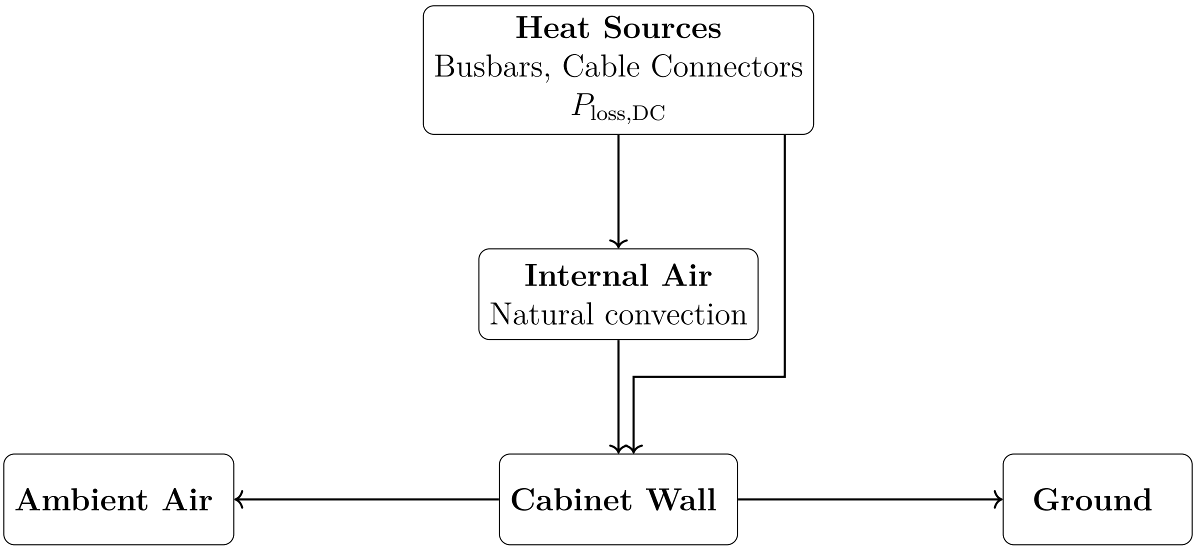

Figure 5.5: Heat flow inside the DC cabinet (same mechanism as AC)

For calculating the temperature of the DC cabinet, exactly the same method that is used in Section 4.3 for the AC cabinet is used here as well. Since the cabinet size, installation conditions, and cooling mechanism have not changed, the same thermal model based on the IEC TR 60890 standard is used.

The only difference compared to the AC case is the total power loss of the system. In the DC cabinet, the total loss is reduced, and the total loss is 146.4 W.

The temperature rise inside the cabinet is calculated as

$$\Delta t_{0.5} = k \cdot d \cdot P^x$$

The coefficients that have not changed compared to the AC case are

$$k = 0.29, \quad d = 1.0, \quad x = 0.804$$

The temperature in the middle part is calculated as

$$\Delta t_{0.5} = 0.29 \times (146.4)^{0.804}$$

$$(146.4)^{0.804} \approx 55.4$$

$$\Delta t_{0.5} \approx 0.29 \times 55.4 \approx 15.3°C$$

This means that the temperature at the middle of the cabinet increases 15.3°C above the ambient temperature.

Temperature Rise at the Top of the Cabinet

The temperature at the top of the cabinet is calculated as

$$\Delta t_{1.0} = c \cdot \Delta t_{0.5}$$

$$c = 1.32$$

$$\Delta t_{1.0} = 1.32 \times 15.3 \approx 20.2°C$$

The temperature generating at the top of the cabinet becomes 20.2°C

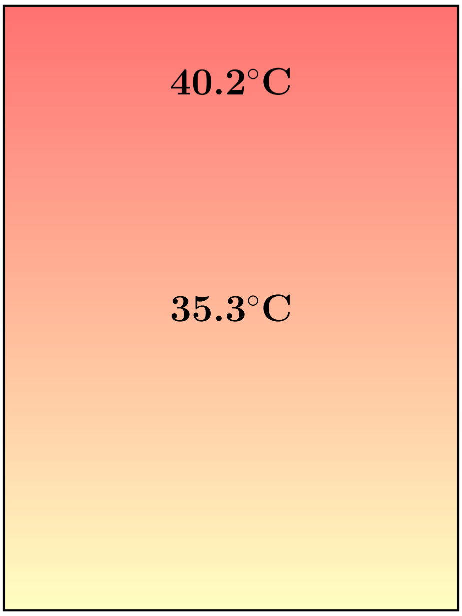

Figure 5.6: Temperature distribution inside the DC cabinet at 1600A

If the ambient temperature is **20°C**, as it shown in figure above, the temperature in the middle of the cabinet is **35.3°C** and the temperature at the top of the cabinet is **40.2°C**.

Based on this result, the power losses in the system have a very important role in the cabinet temperature, and as it can bee seen the temperature at the top of the cabinet is higher than the middle, it is an acceptable and reasonable result, because the thermal mechanism is exactly like this, that heat collects in the upper space.

Temperature under different currents

In this section, it is examined what happens when the current changes occur in the heat of the DC system. Since we know that when the current in the system changes, the losses also change and it directly impacts the system's temperature.

In the previous calculation, the temperatures we calculated was for 1600 A in busbars and connectors. To see how the temperature in the system changes when the current change to, 400 A and 800 A .

When current in the busbars and connectors is 800 A.
The total power loss becomes

$$P = 36.61\,\mathrm{W}$$

The temperature rise for an ambient temperature of 20°C is

$$T_{\text{middle}} \approx 25.02°C$$

$$T_{\text{top}} \approx 26.6°C$$

When current in the busbars and connectors is 400 A.
The total power loss becomes

$$P = 9.15\,\mathrm{W}$$

The final temperature becomes

$$T_{\text{middle}} \approx 21.65°C$$

$$T_{\text{top}} \approx 22.18°C$$

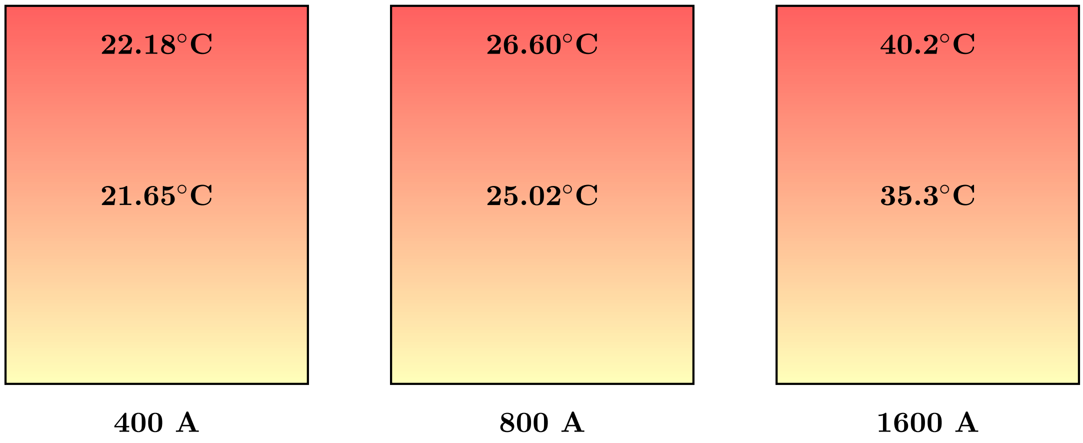

Figure 5.7: Temperature for different current levels in the DC cabinet at 20°C ambient temperature

The result clearly shows that when the current in the DC system increases, it causes higher power losses and higher temperatures inside the cabinet. As it can be seen in the Figure 5.7 according to IEC TR 60890, the relationship between power losses and temperature rise is not linear.

Temperature effect

Season and the ambient temperature have a direct effect on the thermal behavior of the cabinet.

As calculated in the previous sections, the power losses of the DC cabinet is change with ambient temperature. In winter, the losses become lower, while in summer the losses become higher, which directly affects the internal temperature rise of the cabinet.

Winter condition

- Ambient temperature: $T_{\text{amb}} = -20°\text{C}$
- Total power loss: $P_{\text{loss}} = 122.8$ W

The temperature rise generated inside the cabinet is

$$\begin{aligned} \Delta T_{\text{middle}} &= 13.3 \\ \Delta T_{\text{top}} &= 17.5 \end{aligned}$$

The final temperature under winter conditions with an ambient temperature of $-20°\text{C}$ becomes

$$\begin{aligned} T_{\text{middle}} &= -20 + 13.3 = -6.7°\text{C} \\ T_{\text{top}} &= -20 + 17.5 = -2.5°\text{C} \end{aligned}$$

Summer Condition

- Ambient temperature: $T_{\text{amb}} = 30°\text{C}$
- Total power loss: $P_{\text{loss}} = 152.3$ W

The temperature rise generated inside the cabinet due to system losses becomes

$$\begin{aligned} \Delta T_{\text{middle}} &= 15.7 \\ \Delta T_{\text{top}} &= 20.8 \end{aligned}$$

The final temperature under summer conditions with an ambient temperature of $30°\text{C}$ becomes

$$T_{\text{middle}} = 45.7°\text{C}$$
$$T_{\text{top}} = 50.8°\text{C}$$

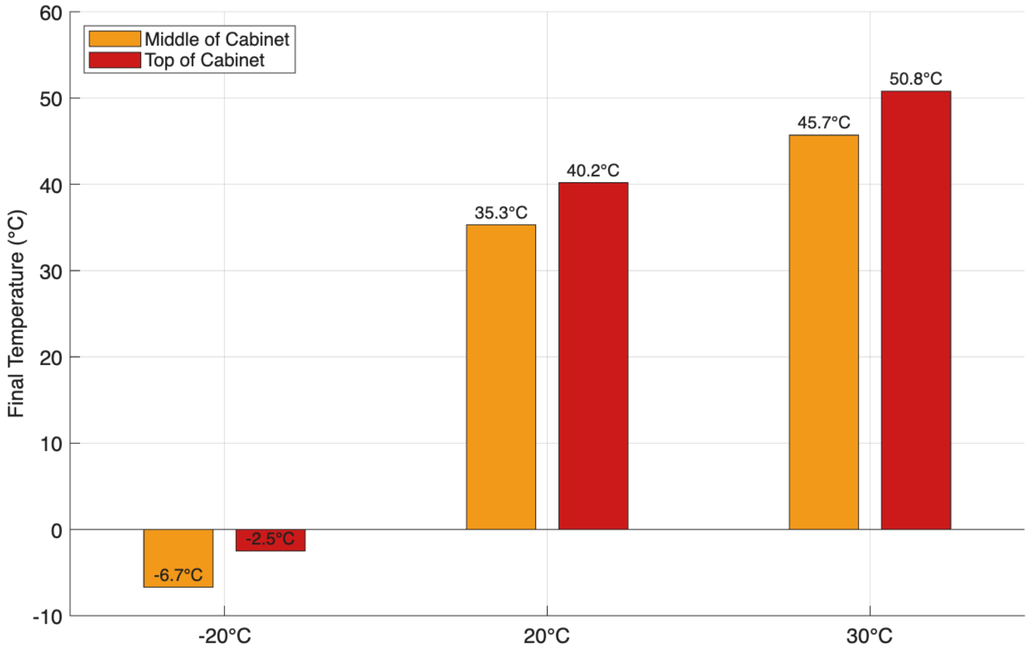

Figure 5.8: DC cabinet temperatures at 1600 under different ambient conditions

As shown in Fig. 5.8, the temperature inside the DC cabinet in winter is between −6°C and −2°C. At an ambient temperature of 20°C, the temperature inside the cabinet is between 36°C and 40°C. In summer, the temperature inside the cabinet is between 45°C and 50°C.

As can be seen in Fig. 5.8, when the ambient temperature changes, it has a direct effect on the DC system, and when Parameters such as the ambient temperature, conductor resistance, and generated power losses change, this directly affects the final temperature of the cabinet or the DC system [16, 17].

Temperature Estimation of Internal Components

The temperature of the individual components, since the current level in the system is the same (1600 A) in the AC cabinet, the components (busbars and cable connectors) are expected to generate exactly the same amount of heat as they did in the AC cabinet.

The final difference in the overall system temperature is due to the different structure of the AC and DC cabinets. In other words, it can be said that because fewer connectors are used in the DC system, the overall heat in the DC case becomes lower than in the AC case. The temperature rise of each busbar at 1600 A is 49.5°C, and for each cable connector is 39.8°C.

5.4 Efficiency of the DC Cabinet

Efficiency is one of the most important parameters for evaluating the performance of an electrical system. Especially when it comes to evaluating or selecting a new DC system, efficiency becomes a very important parameter to consider.

Efficiency describes how much of the input power supplied to the system is delivered to the load and how much is lost inside the system.

One of the factors that has a strong impact on efficiency is the conductor losses. Due to the characteristics of DC systems, the losses in the conductors are lower, which leads to high efficiency of the DC cabinet.

The efficiency can be calculated as

$$\eta = \frac{P_{out}}{P_{out} + P_{loss}}$$

where P_{out} is the transmitted power and P_{loss} is the total electrical loss in the system.

For the DC cabinet, the transmitted power is

$$P_{DC} \approx 1.216\,\mathrm{MW}$$

The total conduction losses are

$$P_{loss,DC} \approx 146.4\,W$$

The DC cabinet efficiency is

$$\eta_{DC} \approx 99.988\%$$

According to the results, the efficiency of the system is very high where its losses are only 0.12% of the transmitted power. This indicates that the system can transfer power with very low losses, due to its DC structure, the DC cabinet is able to deliver electrical power to the load with high efficiency [2, 18].

6

Comparison between AC and DC Cabinet

In this chapter, the comparison between the AC and DC systems is performed based on theoretical scenarios in order to evaluate and compare the behavior of both systems under the same conditions. Therefore, the values and operating scenarios considered in this study are primarily theoretical and may not necessarily represent practical operating conditions that can be implemented in reality.

6.1 Power Comparison

In this section, the power transfer capacity of the AC and DC systems is compared.

This comparison helps to understand how much power can be transferred by the AC and DC cabinets under similar conditions. To understand better the difference between these two systems, the following scenarios are considered.

- Power Transfer Capability of the AC system and DC Systems
- Same transmitted power for the AC system and DC system
- Conductor requirement for a given transmitted power

Power Transfer Capability of the AC and DC Systems

In this condition, both AC and DC systems are in the same condition, meaning they have the same busbar and a current level of 1600 A.

Using Eq. (4.1), the transmitted power in the AC system is

$$P_{AC} \approx 998\,\text{kW}$$

and using Eq. (5.1), the transmitted power in the DC system is

$$P_{DC} \approx 1.216\,\text{MW}$$

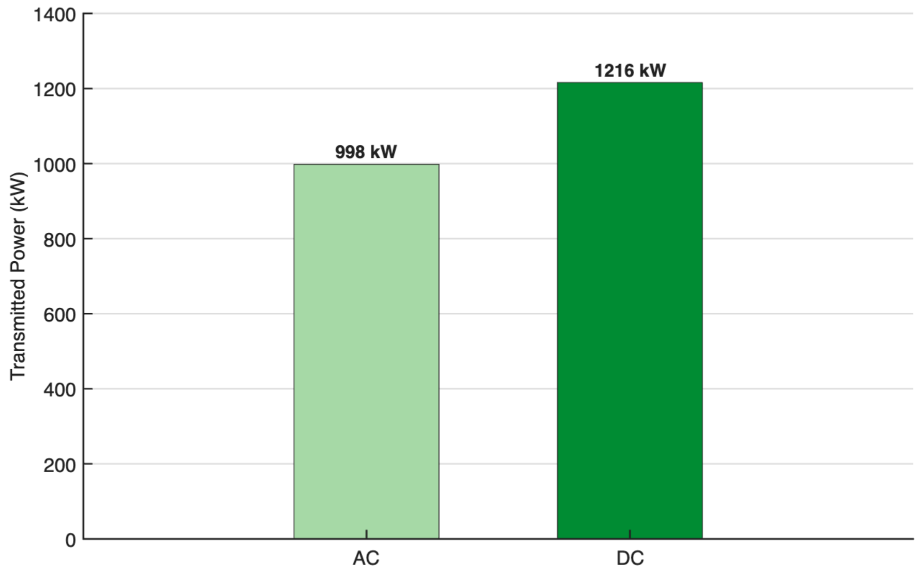

Figure 6.1: AC vs DC transmitted power comparison

This result shows that, under the same current level the DC system can transfer more power (1.216 MW) compared to the AC system (998 kW). The reason is that the AC system includes reactive power and power factor, which leads to a lower transmitted power. Therefore, the DC system can transfer more power, since there is no reactive power or power factor in the DC system.

Same Transmitted Power for the AC and DC Systems

In this section, both systems are going to transfer the same amount of power, equal to the AC system power.

$$P = 998\,\text{kW}$$

For the AC system, to transfer this power, a current of 1600 A is required. For the DC system, the required current can be calculated as

$$I_{DC} = \frac{P}{V_{DC}}$$

$$I_{DC} \approx 1313\,\text{A}$$

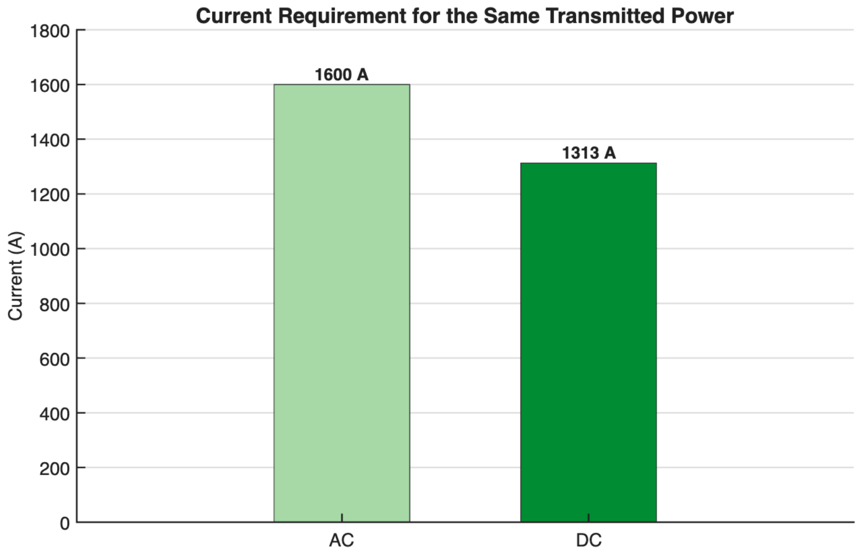

Figure 6.2: AC vs DC current requirement

Results show that, in the DC system, a lower current (1313 A) is required to transfer the same power, which leads to reduction in power losses, a lower current allows the system to use smaller conductor cross-sections, which reduces the material usage and system cost. This is one of the main advantages of the DC system in distribution applications.

Conductor requirement for a given transmitted power

In this section, the required amount of conductors will be analyzed. The AC cabinet uses three active conductors, while the bipolar DC cabinet uses only two active conductors [23].

To transfer a specific power, which was 998.5 kW in the AC system, the two systems need different currents. So the required conductors can be written as

$$\frac{A_{DC,\text{total}}}{A_{AC,\text{total}}} = \frac{2I_{DC}^2}{3I_{AC}^2}$$

where the factor 3 represents the three active conductors in the AC system and the factor 2 represents the two active conductors in the DC system.

$$\frac{A_{DC,\text{total}}}{A_{AC,\text{total}}} = \frac{2(1313)^2}{3(1600)^2} \approx 0.448$$

This means that the reduction in total conductor requirement becomes

$$\text{Reduction} \approx 44.8\%$$

This shows that for 1 MW transmitted power, the DC system can reduce the required conductor cross-section by approximately 44.8%

The cross-sectional area of the DC busbars can be reduced. it can be calculate as

$$A_{DC,\text{per pole}} = A_{AC,\text{per phase}} \cdot \frac{I_{DC}}{I_{AC}}$$

$$\text{Reduction per busbar} \approx 17.94\%$$

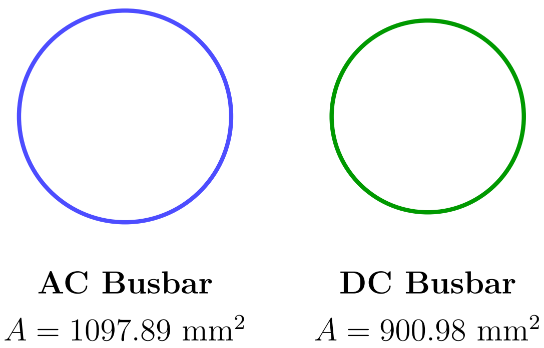

This means that each DC busbar can be made approximately 18% smaller than the AC phase busbar when both systems are designed to transfer 1 MW.

since the AC system has three busbars while the DC system has two busbars, this means that one busbar is eliminated, and each remaining busbar can be reduced about 18%, which results in the total required conductor volume being about 44.8% lower.

This shows that the DC system requires fewer conductors which means that the total losses in the system are lower and the overall system cost is reduced. In addition, using fewer conductors makes the system simpler and can improve its efficiency and lifetime.

In the following comparisons between AC and DC, the comparison is only done based on the components that are common in both systems. These components include the busbars and the cable connectors. This means that the SLI2 fuse-switch disconnector is not considered, because no equivalent component was found for the DC system. The main cross-sectional area of the busbars is considered based on the original cross-sectional area used in the original ABB busbars, which is 1097 mm^2.

6.2 Power Loss Comparison

In this section, the power losses of the AC and DC systems are compared. The goal of this analysis is to determine how power losses behave under different operating conditions. In general, the main source of losses in electrical systems is the resistance of the conductors, and this is directly dependent on the current flowing through the conductors and their resistance. Therefore, as the current or resistance increases, the power losses also increase in the system.

In this part, the main focus is on analyzing the losses in the busbars and the cable conductors, and will be analyzed at different current levels.
The objective of this analysis is to see how the power losses behave under different operating conditions. It becomes clear how much the system losses are when the load is low and also when the system is in overload condition.

For the AC system, the total resistance is

$$R_{\text{total,AC}} = 3\,(R_{\text{busbar}} + R_{\text{connector}})$$

$$R_{\text{total,AC}} \approx 0.0858 \text{ m}\Omega$$

For the DC system, the total resistance is

$$R_{\text{total,DC}} = 2\,(R_{\text{busbar}} + R_{\text{connector}})$$

$$R_{\text{total,DC}} \approx 0.0572 \text{ m}\Omega$$

The results for different current levels are summarized in Table 6.1.

Table 6.1: Power Loss Comparison

Current	**Power Loss AC System (W)**	**Power Loss DC System (W)**
800 A	54.912 W	36.608 W
1600 A	219.648 W	146.432 W
2000 A	343.2 W	228.8 W

As shown in Table 6.1 when current increases, the power losses in both AC and DC systems also increase, this behavior is completely expected. As the values in the table showed, we can compare the performance of the two systems at different current levels.

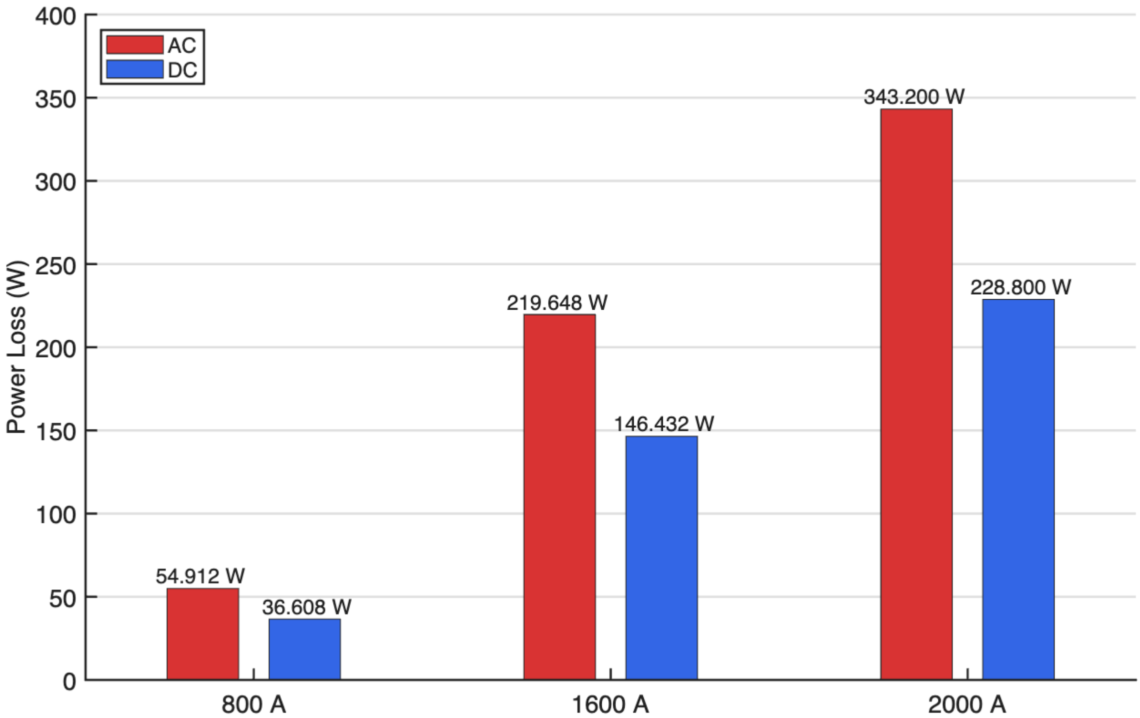

Figure 6.3: AC vs DC power loss comparison

By comparing these values, it becomes clear that in all three operating conditions, the losses in the DC system are lower than in the AC system, and this reduction is approximately 33%. This result shows that, on average, the DC system has about 33% lower losses compared to the AC system.

The main reason for this difference is the system structure of AC and DC. In the AC system, due to the higher number of conductors, then the equivalent resistance of the system is higher. While in the DC system, the number of conductors is lower, which leads in lower system resistance, and this directly leads to reduced losses.

6.3 Thermal Comparison

In this section, the thermal behavior of the AC and DC systems is compared to examine how the temperature changes in both systems under different operating conditions. This thermal comparison is just based on the losses generated in the busbars and cable connectors of the AC and DC systems.

The levels that are considered in this comparison are three current values, 400 A, 800 A, and 1600 A. By selecting these levels, it is possible to examine the thermal performance of the system under conditions where the system load is low, under conditions where the system load is medium, and under nominal conditions when the rated current is drawn from the system. It can be seen how much the temperatures of the AC and DC systems will differ under these conditions.

The temperature results of the two systems under different conditions can be seen in Table 6.2 and Figure 6.4.

Table 6.2: Thermal Comparison between AC and DC Systems

Current	DC Top (°C)	AC Top (°C)	DC Middle (°C)	AC Middle (°C)
400 A	22.18	23	21.65	22.3
800 A	26.02	28.5	25.2	26.5
1600 A	40.20	48.2	35.3	41.4

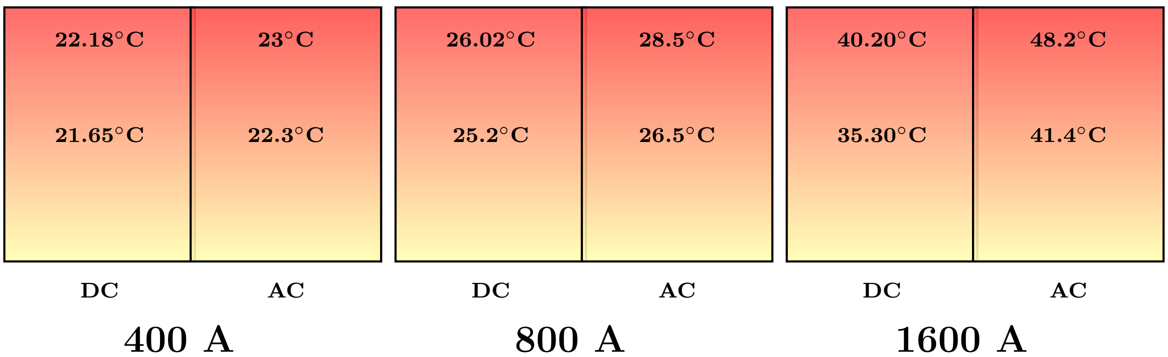

Figure 6.4: Thermal comparison between DC and AC systems at different current levels at 20°C ambient temperature

The result shows that when the current in both systems increases, the temperature in them also increases, which can be directly related to the increase in system power losses.

in all operating conditions, the temperature in the AC system is higher than in the DC system, which is completely expected, since the losses in AC are higher than DC.

As it can bee seen, the temperature at the top of the cabinet is higher than in the middle of the cabinet, which is expected, since this is due to the natural convection mechanism where warm air accumulates at the upper part of an enclosure.

6.4 Efficiency Comparison

In this section, the efficiency of the AC and DC systems is evaluated. It should be noted that in this comparison, due to the absence of components such as fuse switch disconnectors (SLE2) in the DC model, only the components that are common in both systems are considered.

Based on the results of both systems, the total power losses in the AC system are equal to $P_{\text{loss,AC}} = 219.64\,\text{W}$,and in the DC system are equal to $P_{\text{loss,DC}} = 146.4\,\text{W}$. Considering the transmitted power, the efficiency of the AC system is 99.97% and the efficiency of the DC system is 99.98%.

At first glance, the difference in efficiency between these two systems seems very small, but in the long term this difference can become a significant amount in terms of energy. Therefore, to evaluate the difference, the power losses over one year are analyzed.

$$E = P \times t$$

The operating time for one year is

$$t = 8760\,\text{hours/year}$$

The power losses for each system are

$$E_{AC} = 219.64 \times 8760 \approx 1923\,\text{kWh/year}$$

$$E_{DC} = 146.4 \times 8760 \approx 1282\,\text{kWh/year}$$

The energy saving by using the DC system is equal to

$$\Delta E = 641\,\text{kWh/year}$$

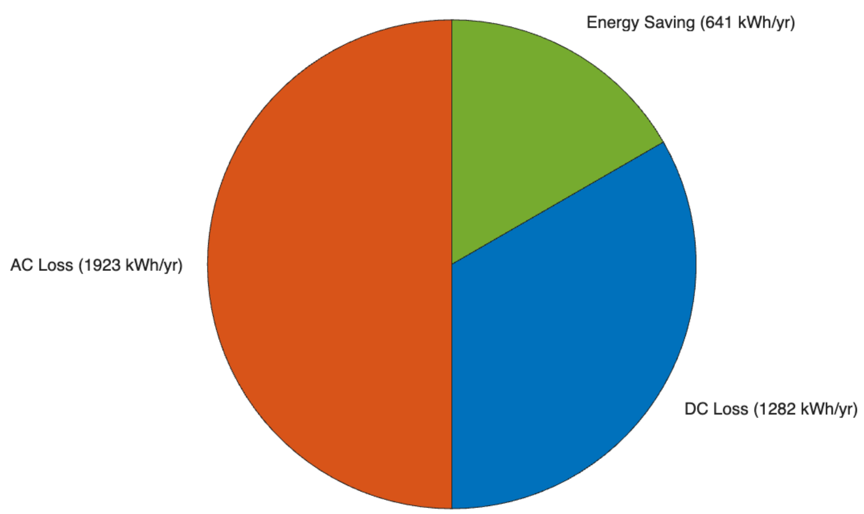

The calculations presented above were performed based on the rated current of 1600 A, which is considered the rated current of this system. However, under normal operating conditions, the cabinet is expected to operate at an average current of approximately 300 A. In this case, the annual energy losses would be around 67.6 kWh/year for the AC system and 45.1 kWh/year for the DC system. Therefore, under these operating conditions, the DC system would provide an annual energy saving of approximately 22.6 kWh/year compared to the AC system.

This result shows that, that the efficiency difference between the AC and DC systems over one year reaches a significant amount of energy. Having a system with higher efficiency, even if the difference is small, has several important consequences.

First, it leads to a reduction in the overall energy losses over time, especially in systems that operate continuously such as low-voltage distribution networks.

Second, lower losses directly affect the thermal behavior of the system. This improves the thermal performance of the system and reduces heat and stress on the equipment, which leads to a longer lifetime of the components.

In addition, from an environmental perspective, improving efficiency reduces the overall energy consumption, which lowers the demand from the power grid and indirectly reduces emissions associated with energy generation and the system becomes more sustainable.

6.5 Cable Structure and Insulation Stress Comparison

In this section, the cable structure and the electrical stresses applied to the insulation are analyzed. In the AC cabinet, as can be seen in the Figure 6.5 and 6.6, the input cables to the cabinet come as four-core cables, consisting of three phases and one neutral, and the output cables of the cabinet can be in two forms, either four-core or five-core. ABB has provided this possibility in the cabinet catalog that the system can be converted from a four-wire configuration to a five-wire configuration.

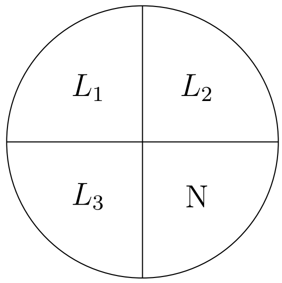

Figure 6.5: Input cable in a three-phase AC system

This AC cabinet is designed for a rated voltage of 400 V and a current of 1600 A. According to the specifications of the cable connectors, the cross-sectional area of the input cables is between 50 mm^2 to 300 mm^2. For this reason, to reach the rated current of 1600 A through this cabinet,multiple cables must be connected in parallel.

In the output section of the AC cabinet, the power distribution is carried out through the fuse switches (SLE2), which can support cable cross-sections between 50 mm^2 and 300 mm^2.

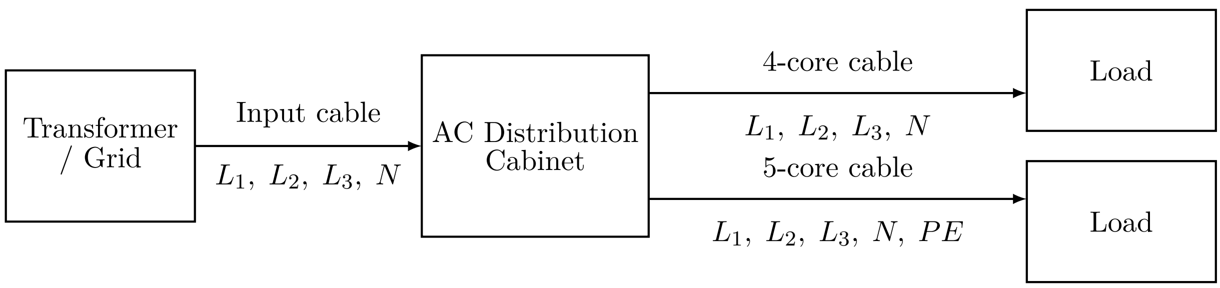

Figure 6.6: AC input/output cable structure

In the DC system, the cable structure is different as it can be seen in the figure 6.7

these cables consist of three conductors, positive pole, negative pole, and neutral and as can be seen in the 6.8 both incoming and outgoing cables are DC.

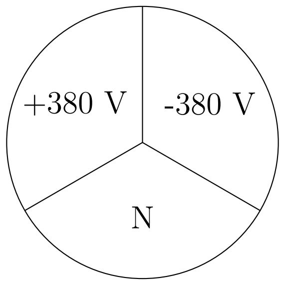

Figure 6.7: DC cable structure

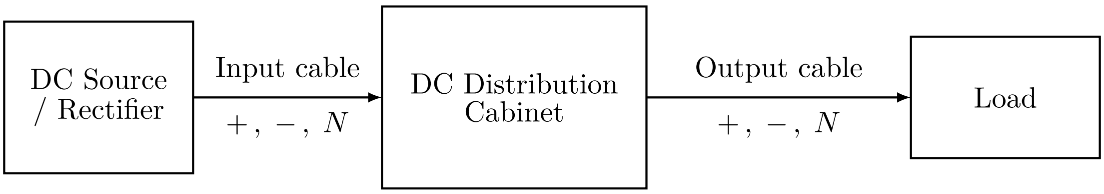

Figure 6.8: DC input/output cable structure

This directly leads to a reduction in the number of conductors compared to the AC system and the amount of material used in DC cables is lower. Over long distances, this reduction has a significant impact on reducing losses and improving the thermal performance of the system. It is also possible to use a smaller cross-sectional area in DC cables to transfer the same power as in AC. Therefore, the total volume of conductive material in the DC system is lower than in the AC system [37].

In the cable structure, the electrical stress applied to the insulation is also different in AC and DC systems. In the AC system, the rated line-to-line voltage is 400 V, and peak value of the voltage calculated as

$$V_{\text{peak,AC}} = \sqrt{2} \times V_{\text{rms}} = \sqrt{2} \times 400 \approx 565\,\text{V}$$

In the DC system, The voltage between each pole and neutral is 380 V, and this voltage is a constant value. This means that the stress for AC cables is about 565 V, while for DC cables it is 380 V. Comparing these two cases shows that the voltage stress in the AC system is significantly higher than in the DC system. Therefore, in the AC system, stronger insulation materials and larger insulation distances are required to prevent electrical breakdown.

Overall, this comparison shows that the DC system has more significant advantages compared to the AC system, both in terms of the number of cables and the amount of conductive materials used, and also in terms of the electrical stress applied to the insulation.

6.6 Safety and Protection

One of the most important challenges in converting an AC cabinet to DC is the protection and safety of the system. In this section, safety and protection in AC and DC systems is studied, and their main differences in terms of protection performance are compared.

In an AC system, the current changes alternately and naturally passes through zero in each cycle. This natural zero-crossing of the current makes it easier to interrupt the current when a fault happens in the system, and also when equipment such as fuse switches, protection switches, or fuses operate, the electric arc is extinguished more easily [41].

In DC systems, the current is in a constant form and there is no natural zero-crossing of the current Therefore, when a fault or a short circuit happens in the system, the fault current increases very quickly. This issue becomes more important when the system is connected to sources such as batteries, capacitors, or power electronic converters because these sources can send their stored energy into the fault path during a fault which makes the fault stronger and harder to control [42].

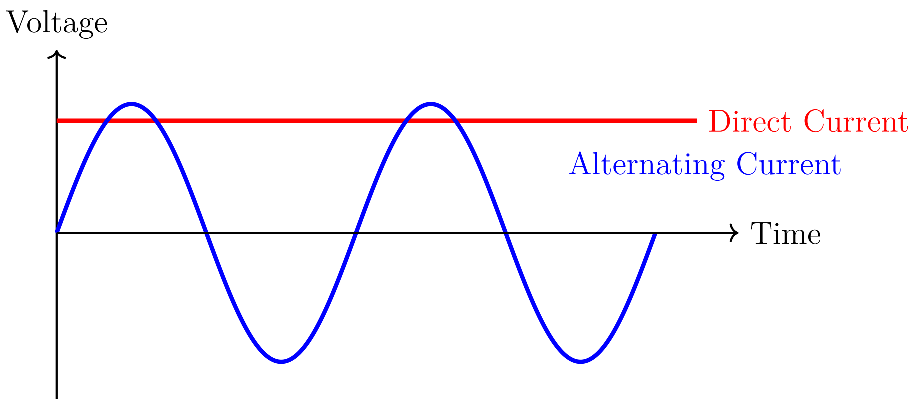

Figure 6.9: Comparison between alternating current and direct current waveforms

The electric arc in DC systems is another challenge. In a DC system, the electric arc is more stable and lasts longer compared to an AC system, and this can cause damage to the contacts, damage to the insulation, and even a risk of fire [43].

In terms of the type of faults, the DC system is also more complex than the AC system. In a bipolar DC structure, a fault can happen between the positive and negative poles, between each pole and neutral, or between each pole and ground therefore, DC protection is not only limited to overcurrent protection [42, 43].

As a result, protection in a DC system is more complex and harder than AC system because of the characteristics of direct current. The main reason is that there is no natural zero-crossing of the current, harder and larger electric arc, fast increase of fault current and the different fault cases in the DC system. This issue can make the system design more complex and increase the cost of protection equipment.

6.7 Environmental Impact Comparison

In addition to the technical and electrical advantages, converting the system from AC to DC also has important environmental impacts, which are mainly related to the reduction of energy losses and lower material consumption in the DC system.

In the previous sections, it was analyzed that the DC cabinet compared to the AC cabinet has lower power losses, and reduced requirement for conductor materials. The yearly power loss for the AC system was calculated to be about 1923 kWh/year and for the DC system 1282 kWh/year, which leads to the conclusion that when the system is converted from AC to DC, about 642 kWh/year, corresponding to approximately 33% reduction in annual power losses, is achieved.

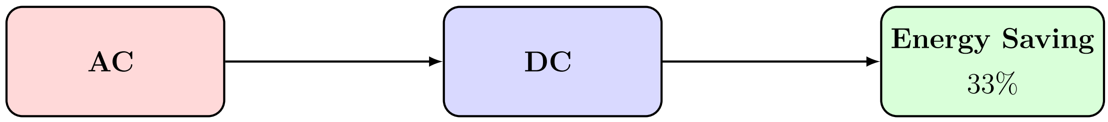

From an environmental point of view, this reduction is very important, because lower losses mean that less power generation is required. Therefore, converting the AC cabinet to DC has a direct impact on the environment. For example, the Ember report shows that the average electricity emissions intensity in the European Union in 2023 was 242 gCO_2/kWh. So, if in this transition 642 kWh/year of losses are reduced, approximately 155 kg of CO_2 is reduced per cabinet per year [38].

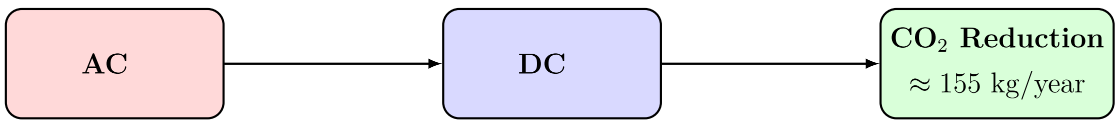

The second important environmental advantage is the reduction of conductor materials. According to the previous calculations, for transmitting the same power, the DC system can reduce the total volume of required conductors around 44.8% compared to the AC system. The production of materials such as copper and aluminum, including the stages of extraction, ore processing, refining, smelting, and transportation, has a significant environmental impact.

For copper production, the cradle-to-gate greenhouse gas emissions are about 3.965 tCO_2 per ton and for aluminum which has much higher emissions about 14.8 tCO_2 per ton. If the requirement for conductors is reduced by 44.8%, the associated climate burden of materials is also reduced approximately by the same proportion. This means that 1.78 tCO_2 per ton for copper and 6.63 tCO_2 per ton for aluminum of material is reduced. This amount of CO_2 reduction has a significant environmental impact [39, 40].

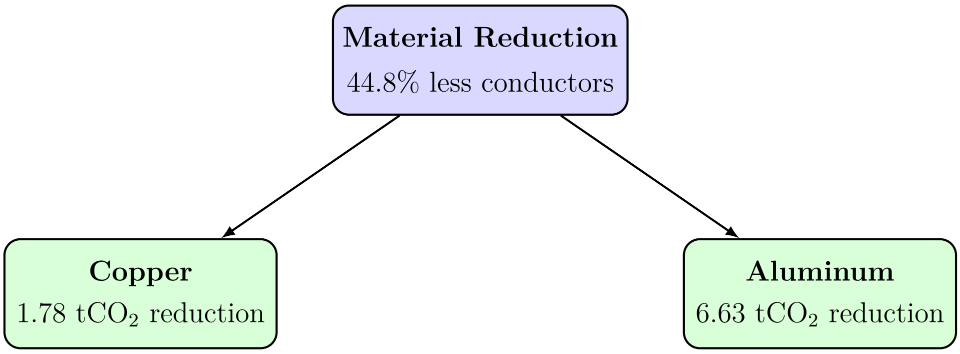

As a result, it can be seen that converting the distribution system from AC to DC has significant environmental advantages. This conversion leads to a reduction in the need for electricity generation and a reduction in the production of conductors.

Finally, it can be stated that the DC system has two very important advantages, improved energy efficiency and reduced material consumption in the production stage. These two factors make the DC system a more sustainable and efficient option compared to the AC system from a life-cycle perspective, especially in large-scale and long-term applications. This difference can play an important role in reducing the overall environmental impact of power distribution systems.

7
Conclusion

In this thesis, the consequences of converting a low-voltage distribution cabinet from an AC system to a DC system are evaluated. This cabinet is a Kabeldon SDC 1673 type from ABB, which is today used for a three-phase AC system with a voltage of 400 V and a rated current of 1600 A, and in this study it is investigated how this cabinet can be converted to a DC bipolar ±380V + N system with a rated current of 1600 A.

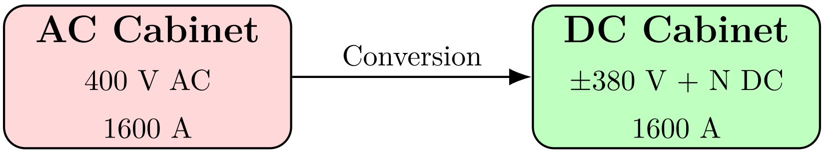

For converting this cabinet from the AC system to the DC system, cases such as power transfer, current level, power losses, thermal behavior, efficiency, protection and safety, and also environmental impacts have been investigated to find out how the performance of this cabinet changes in these parts when it is converted from the AC system to the DC system.

The obtained results show that the proposed DC structure transfers more active power than the AC system with the same rated current. In the AC system, with a line-to-line voltage of 400 V, a rated current of 1600 A, and a power factor of 0.9, the transferred power is about 1 MW. In contrast, in the bipolar DC structure, with a line-to-line voltage of 760 V and a current of 1600 A, the transferred power is about 1.215 MW. The main reason for this increase in power in the DC system is the absence of reactive power. In addition, this bipolar DC structure has more flexibility, because the loads can be connected between each pole and neutral with 380 V, and between the two poles with 760 V.

In the loss section, the results showed that the DC system has lower losses than the AC system. This comparison showed that in the DC system the losses are about 33% lower than in the AC system, and in the thermal section the same trend was also observed. Since the DC system has lower conduction losses, less heat is also generated inside the cabinet. As a result, the internal temperature of the DC cabinet was found to be lower than in the AC cabinet under similar conditions.

In terms of efficiency both systems have very high efficiency because the losses are low compared to the transferred power. However, the efficiency of the DC system was better than that of the AC system. Even though the numerical difference between these two values seemed small, when the system operates continuously during the year, this difference becomes more important. Based on the performed calculations, using the DC structure saves about 642 kWh of energy per year for each cabinet.

AC Cabinet

Power transfer
$P = 998$ kW

Power loss
219 W

Temperature
48°C

Efficiency
99.97%

DC Cabinet

Power transfer
$P = 1.216$ MW

Power loss
146 W

Temperature
40°C

Efficiency
99.98%

From the conductor requirement, the DC system showed an important advantage compared to the AC system. For transferring the same amount of power in the DC system, about 44.8% less conductor material is needed compared to the AC system. This reduction leads to lower material consumption, lower cabinet weight, and lower environmental impact related to the production of conductors. For copper production, the cradle-to-gate CO emissions are around 3.97 tCO per ton, and for aluminum is around 14.8 tCO per ton. 44.8% less conductor material leads to a reduction around 1.78 tCO_2 per ton for copper and about 6.63 tCO_2 per ton for aluminum. Another advantage is the reduction in annual energy losses, where about 642 kWh of energy is saved per year for each cabinet. If this type of system is used in a large number of cabinets, the total effect will be significant. This shows that the DC structure is a more sustainable option compared to the AC system in terms of reducing material consumption and reducing CO2 emissions.

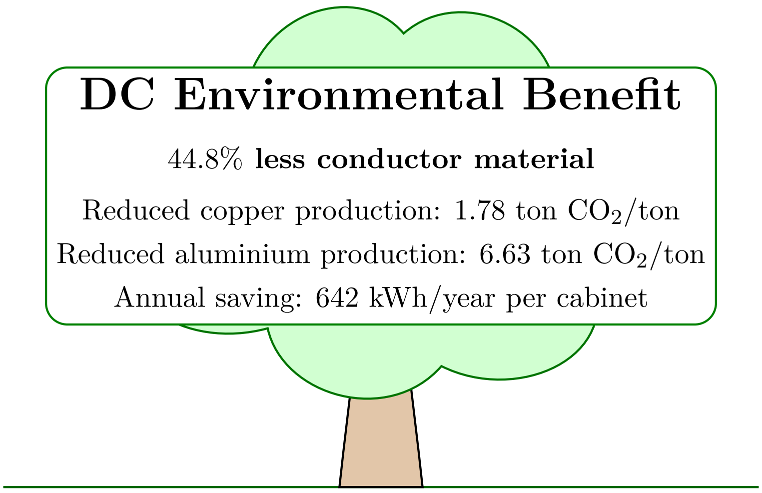

In term of protection and safety, the DC system is more challenging than the AC system. The main reason for this is that DC current does not have a natural zero-crossing. Therefor, the electric arc in the DC system is more stable and longer, and interrupting the fault current is more difficult compared to the case in an AC system. To solve this challenge in this thesis, the OTDC switch-disconnector is proposed as a suitable option for switching and isolation in the DC cabinet. However, installing this equipment on the existing busbars needs a suitable DC adapter, and the final DC adapter was not available and approved in this project. Therefore, the DC protection part remains one of the main limitations for the practical implementation of this cabinet.

Overall, the results of this thesis show that converting a low-voltage distribution cabinet from an AC system to a DC system has significant technical potential. This shows that the DC system can have higher active power, lower power losses, lower heat generation, and higher efficiency compared to the AC system.

In addition, the amount of required conductors in the DC system is reduced, which leads to lower material consumption and lower environmental impact. This result shows that using a DC structure in low-voltage distribution networks can be useful and suitable for applications such as electric vehicle chargers, energy storage systems, renewable sources, data centers, and power-electronic-based loads.

However, converting the AC system to DC still has its own protection challenges, such as protection coordination, fault interruption, electric arc, short circuit, mechanical installation of DC equipment, and this structure needs more development and investigation. Therefore, it can be concluded that converting the AC cabinet to DC is basically possible and promising, and it can be considered as a suitable solution for future distribution networks.

Bibliography

[1] T. Dragicevic, X. Lu, J. C. Vasquez, and J. M. Guerrero, "DC Microgrids—Part I: A Review of Control Strategies and Stabilization Techniques," *IEEE Transactions on Power Electronics*, 2015. Available: `https://www.researchgate.net/publication/283180934_DC_Microgrids-Part_I_A_Review_of_Control_Strategies_and_Stabilization_Techniques`

[2] F. Zhang et al., "Advantages and Challenges of DC Microgrid for Commercial Building: A Case Study from Xiamen University DC Microgrid," IEEE, 2015. Available: `https://doi.org/10.1109/ICDCM.2015.7152068`

[3] V. A. Prabhala, B. P. Baddipadiga, P. Fajri, and M. Ferdowsi, "An Overview of Direct Current Distribution System Architectures & Benefits," *Energies*, vol. 11, no. 9, p. 2463, 2018. Available: `https://doi.org/10.3390/en11092463`

[4] S. Kim and H. Jeon, "Comparative Analysis on AC and DC Distribution Systems for Electric Propulsion Ship," *Journal of Marine Science and Engineering*, vol. 10, no. 5, p. 559, 2022. Available: `https://doi.org/10.3390/jmse10050559`

[5] H. E. Gelani, F. Dastgeer, K. Siraj, M. Nasir, K. A. K. Niazi, and Y. Yang, "Efficiency Comparison of AC and DC Distribution Networks for Modern Residential Localities," *Applied Sciences*, vol. 11, no. 1, p. 144, 2021. Available: `https://www.mdpi.com/2076-3417/9/3/582`

[6] P. Ollas, *Energy Savings Using a Direct Current Distribution Network in a PV and Battery Equipped Residential Building*, Licentiate Thesis, Chalmers University of Technology, Gothenburg, Sweden, 2020. Available: `https://research.chalmers.se/publication/515531/file/515531_Fulltext.pdf`

[7] H. E. Gelani, M. Nasir, F. Dastgeer, and H. Hussain, "Efficiency Comparison of Alternating Current (AC) and Direct Current (DC) Distribution System at Residential Level with Load Characterization and Daily Load Variation," *Proceedings of the Pakistan Academy of Sciences: A. Physical and Computational Sciences*, vol. 56, no. 3, pp. 1–12, 2019. Available: `https://www.researchgate.net/publication/319481270_Efficiency_comparison_of_alternating_current_AC_and_direct_current_DC_distribution_system_at_residential_level_with_load_characterization_and_daily_load_variation`

[8] M. Amin, Y. Arafat, S. Lundberg, and S. Mangold, "Low Voltage DC Distribution System Compared with 230 V AC," in *IEEE Electrical Power and Energy Conference (EPEC)*, 2011. `https://doi.org/10.1109/EPEC.2011.6070222`

[9] SparkFun Electronics, “Alternating Current (AC) vs. Direct Current (DC),” [Online]. Available: https://learn.sparkfun.com/tutorials/alternating-current-ac-vs-direct-current-dc/all

[10] M. A. V. Rasmussen, T. M. Andersen, and M. G. Simonsen, “A comparative analysis of system efficiency for AC and DC residential power distribution paradigms,” *Energy and Buildings*, vol. 138, pp. 273–282, 2017. https://doi.org/10.1016/j.enbuild.2016.12.077

[11] M. Noritake, K. Shimizu, and T. Ise, “Low voltage DC distribution system compared with 230 V AC,” in *Proc. IEEE Electrical Power and Energy Conference (EPEC)*, 2011. https://doi.org/10.1109/EPEC.2011.6070222

[12] L. L. Grigsby, *The Electric Power Engineering Handbook*, 2nd ed., Boca Raton, FL, USA: CRC Press, 2007. Available: https://www.energy-community.org/dam/jcr:6e2f515e-59e7-40b8-926a-ad047d1902e2/Power%20Systems%20-%20Electric%20Power%20Engineering%20Handbook,%20Second%20edition%20.pdf

[13] Mingchele Engineering, “3 Phase Voltage Calculation and Power Formula,” [Online]. Available: https://www.mingchele.com/blog/industry-knowledge/3-phase-voltage-calculation/

[14] Engineering Toolbox, “Convective Heat Transfer,” [Online]. Available: https://www.engineeringtoolbox.com/convective-heat-transfer-d_430.html.

[15] ABB, "ABB Kabeldon Enclosures – Safe and reliable installations," Product Catalogue, 2019.

[16] B. Andersson, *Lumped Parameter Thermal Modelling of Electric Machines: Analysis of an Interior Permanent Magnet Synchronous Machine for Vehicle Applications*, Master’s thesis, Chalmers University of Technology, Gothenburg, Sweden, 2013. Available: Available: https://odr.chalmers.se/server/api/core/bitstreams/608ffd7a-4c70-499d-92e8-b9f8bff4545d/content

[17] S. Touhami, Y. Bertin, Y. Lefèvre, J. F. Llibre, C. Henaux, and M. Fénot, “Lumped Parameter Thermal Model of Permanent Magnet Synchronous Machines,” in *Proc. Electrimacs*, Toulouse, France, Jul. 2017. Available: https://www.researchgate.net/publication/318348628_Lumped_Parameter_Thermal_Model_of_Permanent_Magnet_Synchronous_Machines

[18] D. Nilsson, *DC Distribution Systems*, Licentiate Thesis, Department of Energy and Environment, Chalmers University of Technology, Gothenburg, Sweden, 2005. Available: https://webfiles.portal.chalmers.se/et/Lic/NilssonDanielLic.pdf

[19] ABB, “Fuse switch disconnector 6305.0107.1,” [Online]. Available: https://new.abb.com/products/6305.0107.1

[20] ABB, “Cable distribution cabinet 6330.0555.0,” ABB Product Page, [Online]. Available: https://new.abb.com/products/6330.0555.0.

[21] ABB, “KSFS-1698 phase busbar for Kabeldon distribution system,” ABB Product Page, [Online]. Available: https://new.abb.com/products/2CGD000790P1264/ksfs-1698.

[22] ABB, “ADI 300 insulated connector (Product ID: 2CGD000503A1000),” ABB Product Page, [Online]. Available: https://new.abb.com/products/2CGD000503A1000/adi-300.

[23] M. Starke, L. Tolbert, and B. Ozpineci, "AC vs. DC Distribution: A Loss Comparison," [Online]. Available: https://www.dut.ac.za/wp-content/uploads/2019/05/AC-vs.-DC-distribution-A-Loss-Comparison.pdf.

[24] ABB, "KSST 316/23 busbar support (Product No. 5332.0106.0)," ABB Product Page, [Online]. Available: https://new.abb.com/products/5332.0106.0.

[25] "Thermal Study of LV Electric Switchboards," [Online]. Available: https://kh.aquaenergyexpo.com/wp-content/uploads/2023/12/Thermal-Study-Of-LV-Electric-Switchboards.pdf.

[26] Siechem Technologies, "Conductor Resistance," [Online]. Available: https://www.siechem.com/wp-content/uploads/2017/02/conductor-Resistance.pdf.

[27] Electrical World, "Electrical Resistance and How to Calculate It," [Online]. Available: https://electrical-world.com/posts/electrical-resistance-and-how-to-calculate-it.

[28] N. Padmanabhan, "A Transient Thermal Model for Power Electronics Systems," arXiv preprint arXiv:2403.03268, 2024. Available: https://arxiv.org/pdf/2403.03268.

[29] International Electrotechnical Commission (IEC), "A method of temperature-rise verification of low-voltage switchgear and controlgear assemblies by calculation," IEC TR 60890, Edition 3.0, 2022.

[30] ABB, "SLE Fuse Switch Disconnector Leaflet," ABB, 2019. [Online]. Available: https://library.e.abb.com/public/312def2f7f17418ba18d48d5c7fb6e34/SLE_leaflet_2CGC0129_revB.pdf.

[31] ABB, "Introduction to Direct Current Applications," ABB Electrification, Technical Training Document, 2020. [Online]. Available: https://mylearning.abb.com/config/mylearning.abb.com/sites/default/files/fileupload/1600843991-introduction-to-direct-current-applications-6PnKizkN.pdf.

[32] ABB, "DC switch-disconnectors (16–1600 A)," ABB Electrification, [Online]. Available: https://new.abb.com/low-voltage/products/switches/dc-switch-disconnectors-16-1600-a.

[33] *Low-voltage switchgear and controlgear – Part 1: General rules*, International Electrotechnical Commission (IEC), IEC 60947-1, Edition 6.0, Geneva, Switzerland, 2020. (Used as reference in ABB design practice)

[34] Ifö Electric AB, "HICAP ECO NH Fuse Links – Technical Data," Ifö Electric, Sweden.

[35] P. Kumar, R. K. Singh, and R. Mahanty, "Minimum Phase Bipolar Converter for DC Microgrid Applications," *IET Power Electronics*, vol. 13, no. 1, pp. 178–190, 2020. Available: https://ietresearch.onlinelibrary.wiley.com/doi/10.1049/iet-pel.2019.0170.

[36] J. O. Lee, Y. S. Kim, and J. H. Jeon, "Generic Power Flow Algorithm for Bipolar DC Microgrids Based on Newton–Raphson Method," *International Journal of Electrical Power & Energy Systems*, vol. 142, p. 108357, 2022. Available: https://doi.org/10.1016/j.ijepes.2022.108357.

[37] T. Thiringer, M. Bahmani, A. Manikoff, J. Söderbom, M. Kharezy, H. Hagmar, and A. Lindskog, "Förstudie av förlustbesparingspotential via användande av högfrekvenstransformator och likspänningsdistribution," E2B2 Report, Energimyndigheten, Sweden.

[38] Ember, "European Electricity Review 2024: EU Electricity Trends," [Online]. Available: https://ember-energy.org/latest-insights/european-electricity-review-2024/eu-electricity-trends/.

[39] International Copper Association (ICA), "Life Cycle Inventory (LCI) Global Summary for Copper Production," International Copper Association, 2023. [Online]. Available: https://internationalcopper.org/wp-content/uploads/2023/05/ICA-LCI-GlobalSummary-202305-F.pdf.

[40] International Aluminium Institute (IAI), "Global aluminium industry greenhouse gas emissions intensity reduction continues with total emissions below 2020 peak," [Online]. Available: https://international-aluminium.org/global-aluminium-industry-greenhouse-gas-emissions-intensity-reduction-continue

[41] F. Mohan and N. Sasidharan, "Protection of low voltage DC microgrids: A review," *Electric Power Systems Research*, vol. 225, p. 109822, 2023. [Online]. Available: https://doi.org/10.1016/j.epsr.2023.109822

[42] S. Augustine, J. E. Quiroz, M. J. Reno, and S. Brahma, "DC Microgrid Protection: Review and Challenges," Sandia National Laboratories, Sandia Report SAND2018-8853, Aug. 2018. [Online]. Available: https://www.osti.gov/servlets/purl/1465634.

[43] P. Salonen, P. Nuutinen, J. Partanen, and P. Peltoniemi, "Protection scheme for an LVDC distribution system," in *Proc. CIRED 20th Int. Conf. on Electricity Distribution*, Prague, Czech Republic, Jun. 2009, Paper 0891. [Online]. Available: https://www.researchgate.net/publication/224593782_Protection_scheme_for_an_LVDC_distribution_system.

[44] ABB, "OT and OTDC Switch-Disconnectors for DC Applications," ABB Electrification, Product document, Jun. 2024. [Online]. Available: https://library.e.abb.com/public/eb44e9a6f3ee422589052faf4980954f/1SCC301023C0201_DC20%20OT_-135_VIDEO_06_2024.pdf.

A
Appendix 1

DEPARTMENT OF SOME SUBJECT OR TECHNOLOGY
CHALMERS UNIVERSITY OF TECHNOLOGY
Gothenburg, Sweden
www.chalmers.se

CHALMERS
UNIVERSITY OF TECHNOLOGY